CERN Academic Training Lectures
April 20-21 and 22, 2009

"The Use of Physics Detectors in Medicine. The Future of Molecular Imaging and Multimodality Imaging"

Alberto Del Guerra
Department of Physics "E.Fermi"
University of Pisa, and INFN, Sezione di Pisa
56127 Pisa, Italy

e_mail: alberto.delguerra@df.unipi.it
http://www.df.unipi.it/~fiig/

FIIG FUNCTIONAL IMAGING AND INSTRUMENTATION GROUP
UNIVERSITY OF PISA

CERN Academic Training Programme

Lecture #3 - *22 April 2009*

"The Future of Molecular Imaging and Multimodality Imaging: advantages and technological challenges."

Contents

- **New Solid State Photo-Detectors (SiPM)**
- **PET-MR**
- **PET on-line in Hadrontherapy**
- **Conclusions**

NEW SOLID STATE PHOTODETECTORS

Silicon PhotoMultiplier = SiPM
The Ultimate dream??

SOLID STATE PHOTODETECTOR➔

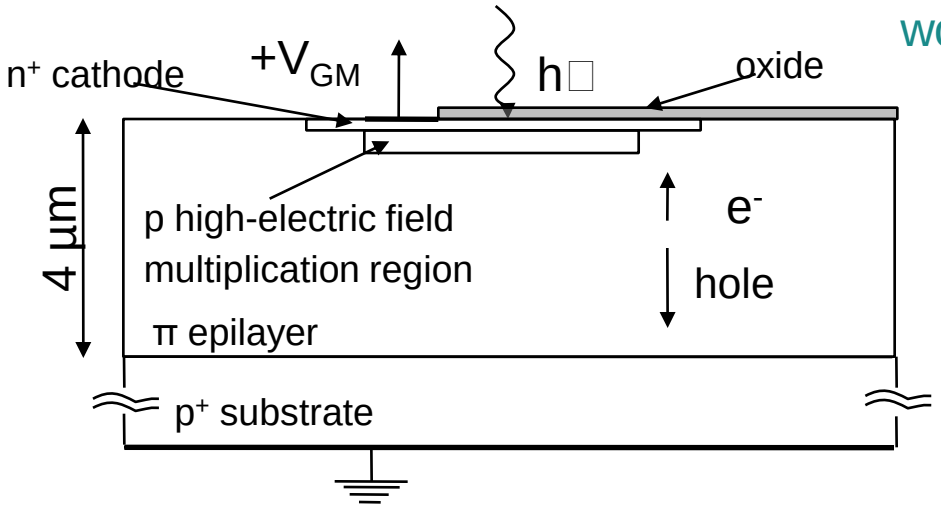

-The photon is absorbed and generates an electron/hole pair

-The electron/hole diffuses or drifts to the high-electric field multiplication region

-The drifted charge undergoes impact ionization and causes an avalanche breakdown.

-Resistor in series to quench the avalanche (limited Geiger mode).

As produced at FBK-irst,Trento, Italy➔

SiPM: **Multicell Avalanche Photodiode** working in limited Geiger mode

- 2D array of microcells: structures in a common bulk.
- Vbias > Vbreakdown: high field in mult. region
- Microcells work in Geiger mode: the signal is independent of the particle energy
- The SiPM output is the sum of the signals produced in all microcells fired.

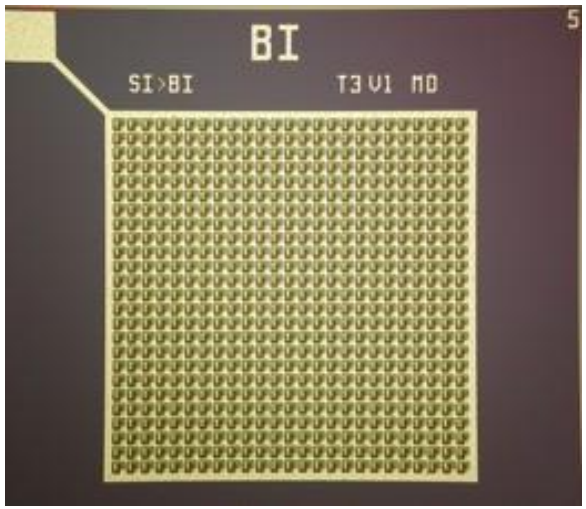

➔High gain ➔Low noise ➔ Good proportionality if $N_{photons} << N_{cells}$

Results: characterization

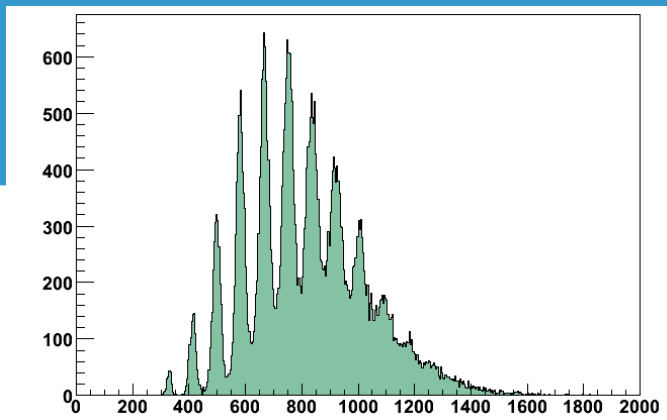

Collaboration with FBK- irst (Trento, Italy), that is developing SiPMs since 2005:

First detectors - Single SiPMs (2006)

First matrices 2x2 (2007)

First matrices 4x4 (2008)

First matrices 8x8 (2009)

Breakdown voltage V_B ~ 30V**, very good uniformity.**

Single photoelectron **spectrum: well resolved peaks.**

Gain: ~10^6

- Linear for a few volts over V_{BD}.
- Related to the recharge of the diode capacitance C_D from V_{BD} to V_{BIAS} during the avalanche quenching.
  G=(VBIAS-VB) x C_D/q

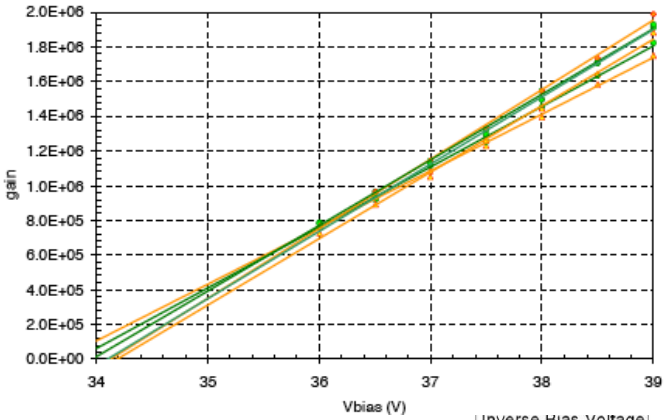

Dark rate:

- 1-3 MHz at 1-2 photoelectron (p.e.) level, ~kHz at 3-4 p.e (room temperature).
- Not a concern for PET applications.

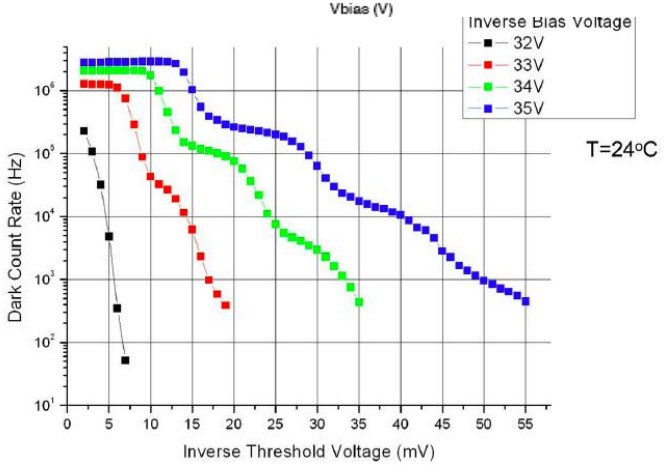

Results: intrinsic timing

Intrinsic timing measured at s.p.e level:
60 ps (σ) for blue light at 4V overvoltage.

SiPM illuminated with a pulsed laser with 60 fs pulse width and 12.34 ns period, with less than 100 fs jitter.

Two wavelengths measured:

λ = 400 ± 7 nm and λ = 800 ± 15 nm.

Time difference between contiguous pulses is determined.

The timing decreases with the number of photoelectrons as

1/√(Npe)➔ 20 ps at 15 photoelectrons.

[G. Collazuol et al., VCI 2007, NIM A 2007, A581, 461-464]

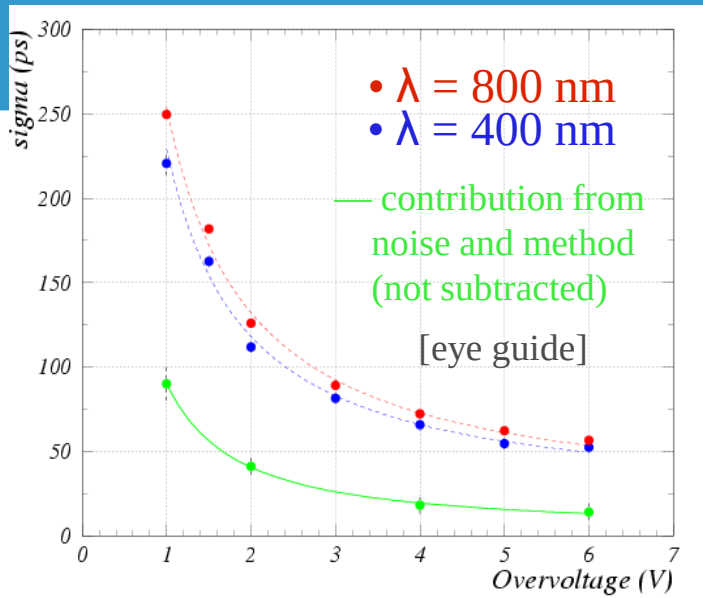

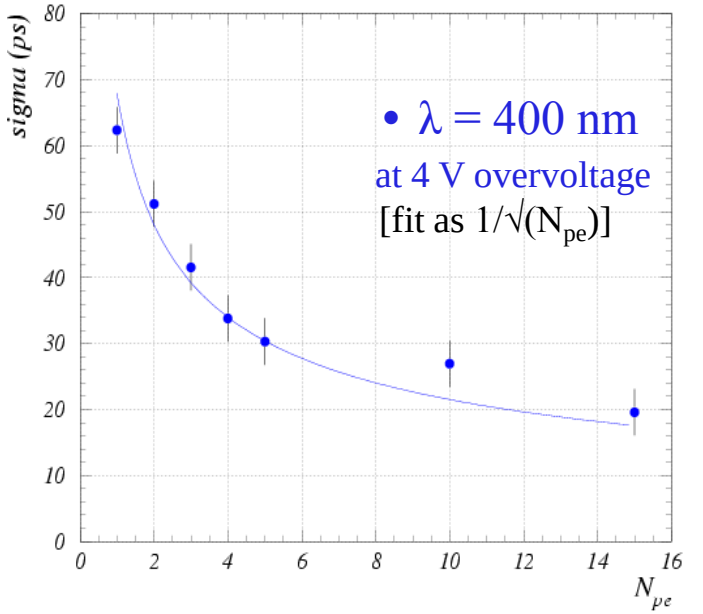

Results: coincidence timing (TOF)

Coincidence measurement with two LSO crystals (1x1x10 mm^3) coupled to two SiPMs {From Theory: **Post and Schiff. Phys. Rev. 80 (1950)1113.**}

$$\sigma \sim \frac{\sqrt{Q}\,\tau}{< N >}$$

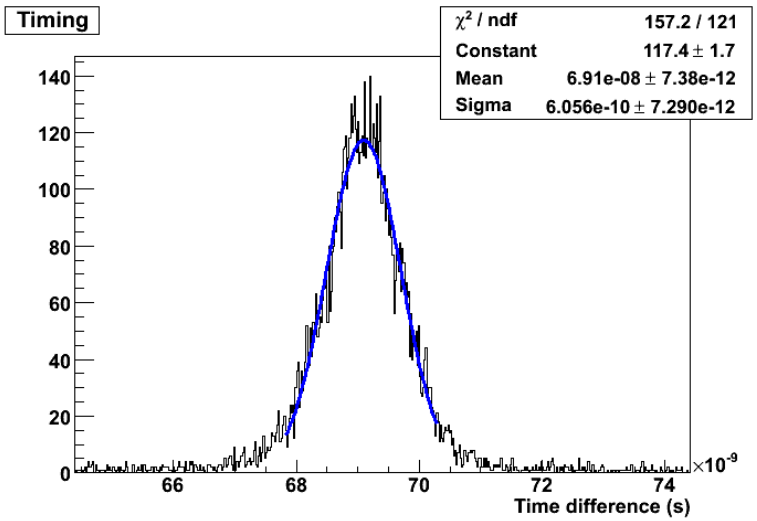

Where:

<N> = average number of photons: ~ 100 photons at the photopeak

Q = Trigger level: ~1 photoelectron.

τ = Decay time of the scintillator

For two scintillators in coincidence expected : => $\sqrt{2}\sigma$~ 630 ps .

Measured => ~ 600 ps sigma.

Measurements in agreement with what we expect!!

[G.Llosa,et al., IEEE Trans. Nucl. Sci. 2008, 55(3), 877-881.

Results: energy resolution (DE/E)

Setup:

- 2 LSO [1mm x 1mm x 10mm] crystals coupled to 2 SiPMs
- Home made amplifier board.
- Time coincidence of signals.
- VME QDC for DAQ.
- ^{22}Na source.

Energy resolution in coincidence: 20% FWHM.
(best result: 17.5 %)

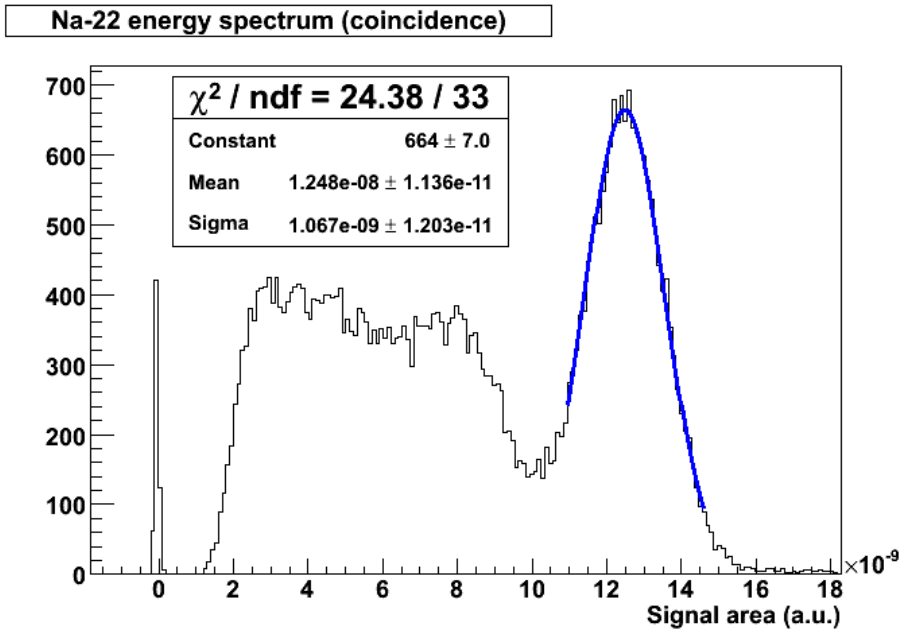

[G.Llosa et al, IEEE Trans. Nucl. Sci. 2008, 55(3), 877-881.]

Results: New detectors (May 2007)

Different geometry,size,microcell size and GF.

40x40μm² => GF 44%
50x50μm² => GF 50%
100x100μm² => GF 76%

circular

1mm ϕ 1x1mm² 2x2mm² 3x3mm² (3600 cells) 4x4mm² (6400 cells)

Matrices 16 elements (4x4)

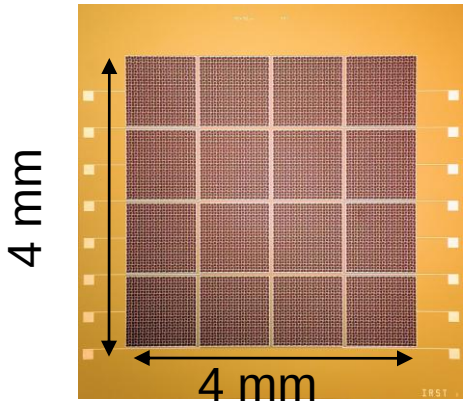

IV CURVES OF 9 MATRICES.

VERY UNIFORM BREAKDOWN POINT

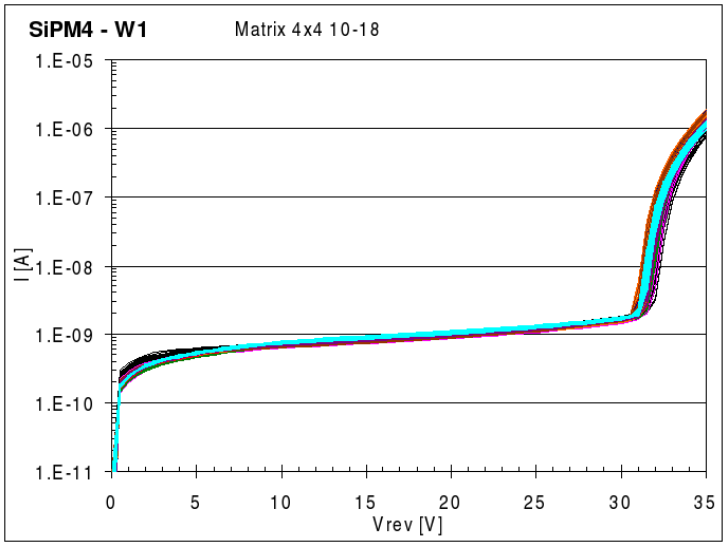

[C.Piemonte et al, Il Nuovo Cimento C, 2007,30(5),473-482]

SiPM 4x4 matrices from FBK-irst

Composed of 16 (4x4) pixel elements in a common substrate
1 mm pixels in 1.06 mm pitch

- Structure: n^+-p-π -p^+ optimized for blue light: Shallow n^+ layer + specific antireflective coating.
- Each pixel: 625 (25 x 25) microcells, 40μm x 40μm size.
- Polysilicon quenching resistor.
- Fill factor 44%.

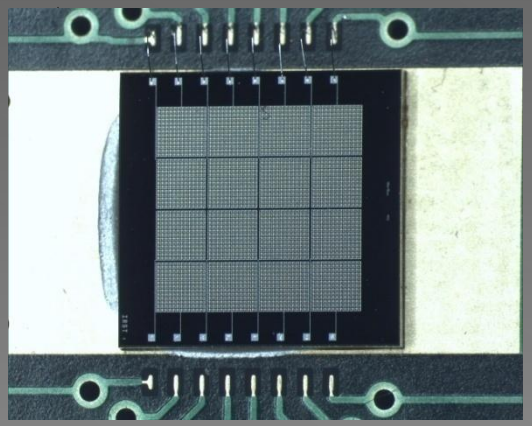

Bonded SiPM array

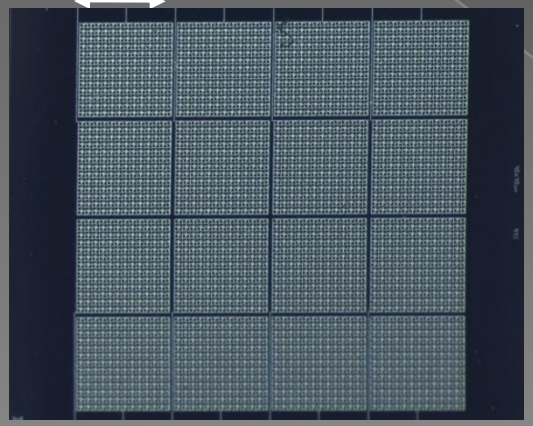

SiPM array

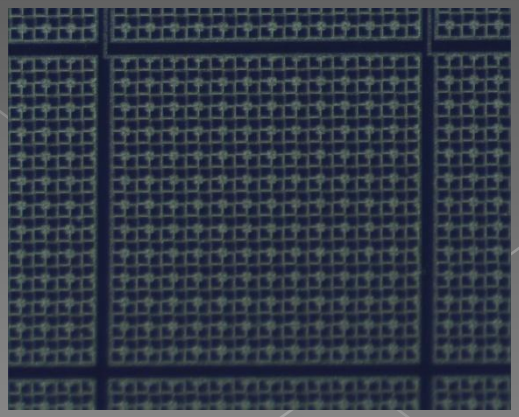

SiPM pixel

4x4 Matrices Characterization

- The full characterization of the first production was performed at LAL, Orsay.
- Excellent uniformity.
  - Breakdown voltage 30.5V ; σ_{var}= 0.5%
  - Gain @33V 1.46x10^6 ; σ_{var}= 4%
- Mean dark rate @33V (ΔV=2.5V): 1.98 MHz
- PDE @ 33V 8-10% from 420 to 680 nm wavelength.

Expected PDE >15% for the results shown here (run II and ΔV=4V)

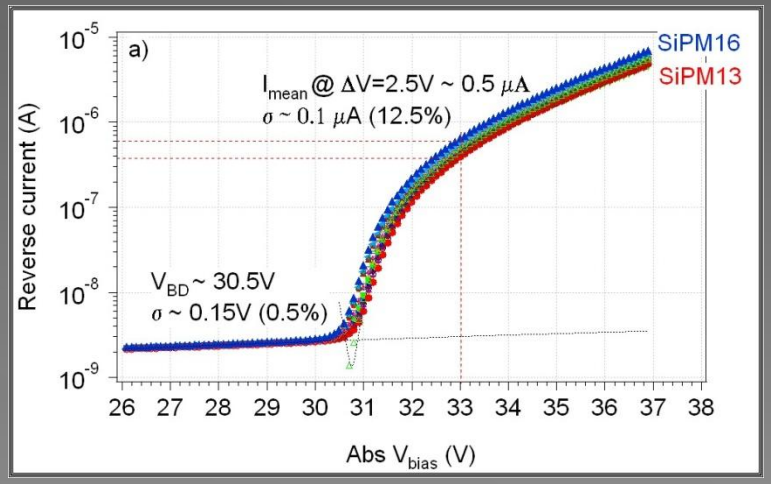

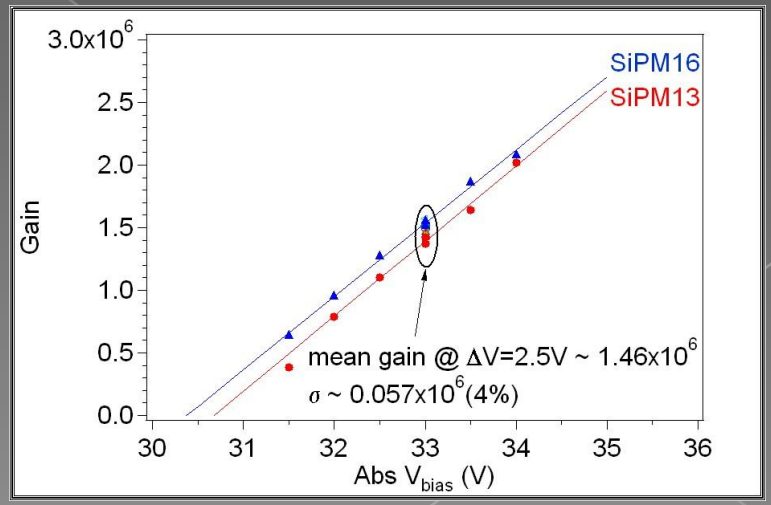

N. Dinu et al., Pixel 2008 workshop,,Fermilab, September 2008.

Readout: MAROC2 ASIC

- Developed at Laboratoire de l'Accelerateur Lineaire, Orsay.
- 64 channels
- low noise preamplifier with variable gain (6 bits)
- Slow shaper (~20-150 ns, adjustable)
- Fast shaper (15 ns) + 3 discriminators =>Trigger signal.
- Designed for MAPMT (H8500)– not optimized for SiPMs, but allows us to make the tests satisfactorily.

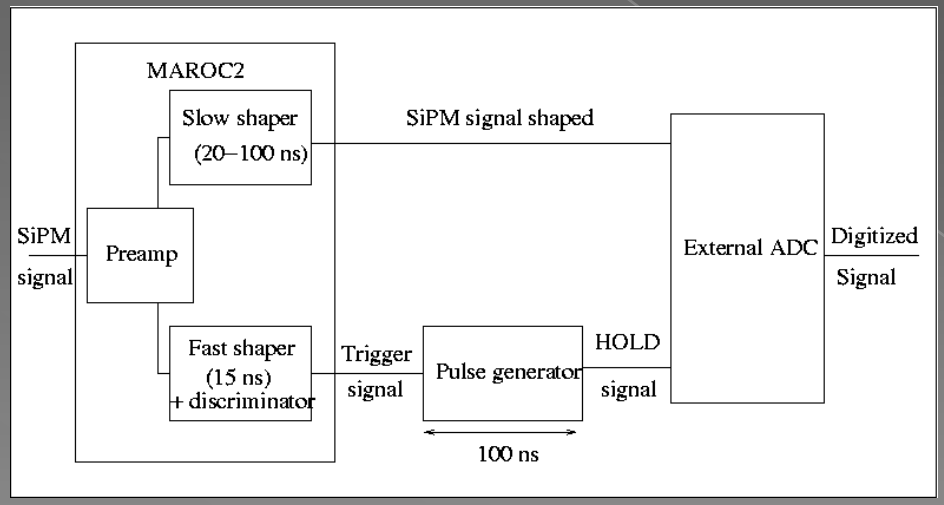

Readout: Test board

- Altera FPGA
- USB Port
- ADC on the board.
- ASIC calibration input.
- LabVIEW software for data acquisition

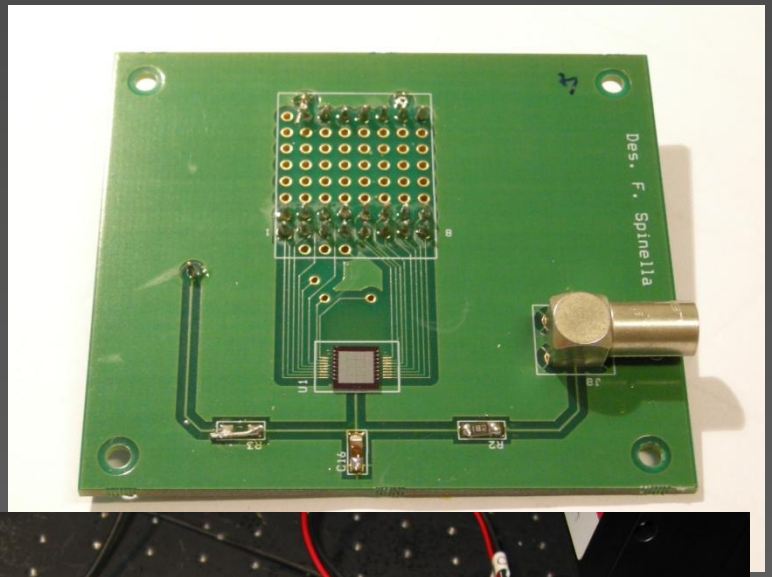

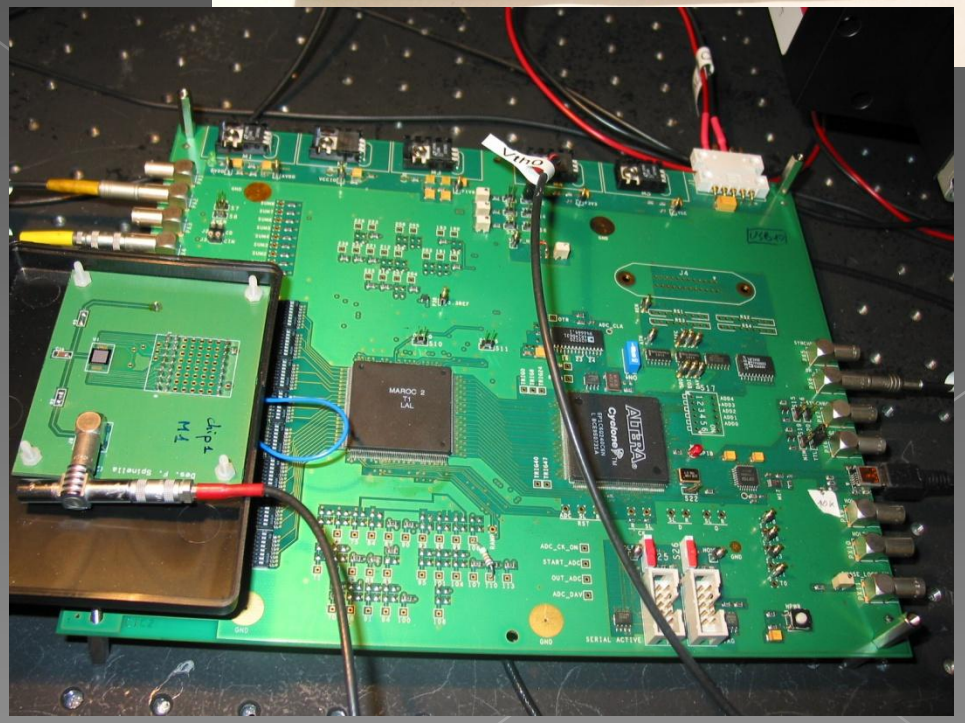

Position determination

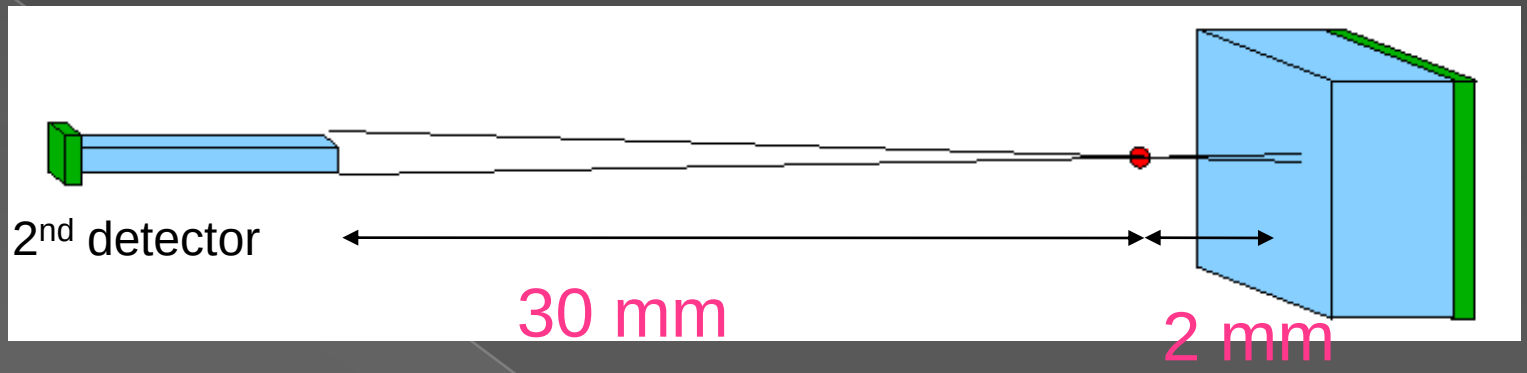

- Coincidence with a 2nd detector: 1 mm x 1 mm x 1 cm crystal coupled to a SiPM
- Source close to the matrix, far from 2nd detector
- Move together source and 2nd detector.

Position determination setup

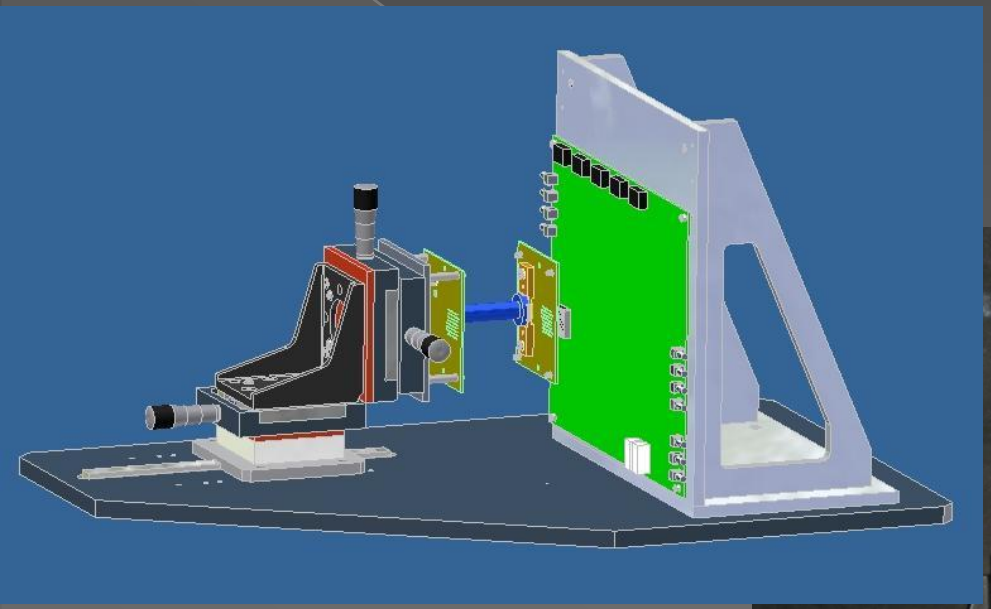

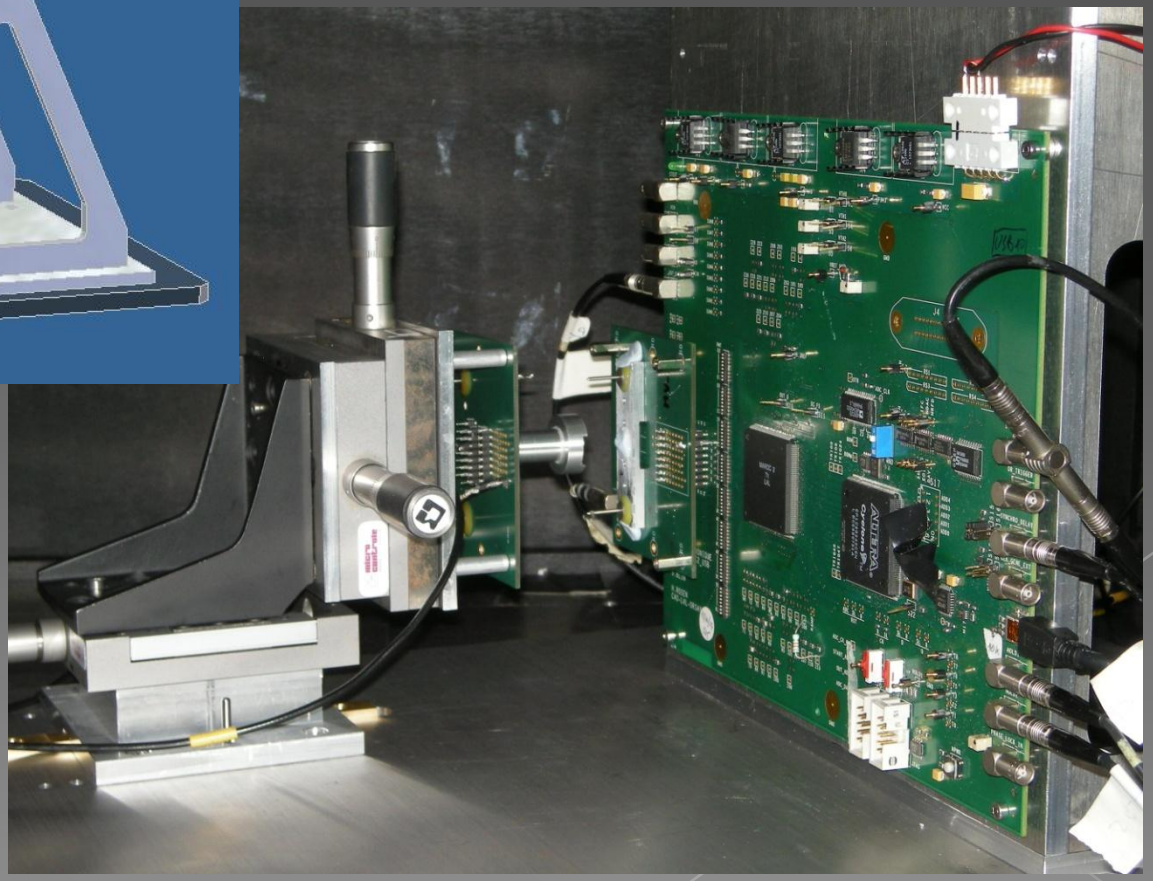

Position determination- crystal array

Hitmap for different source positions with crystal array

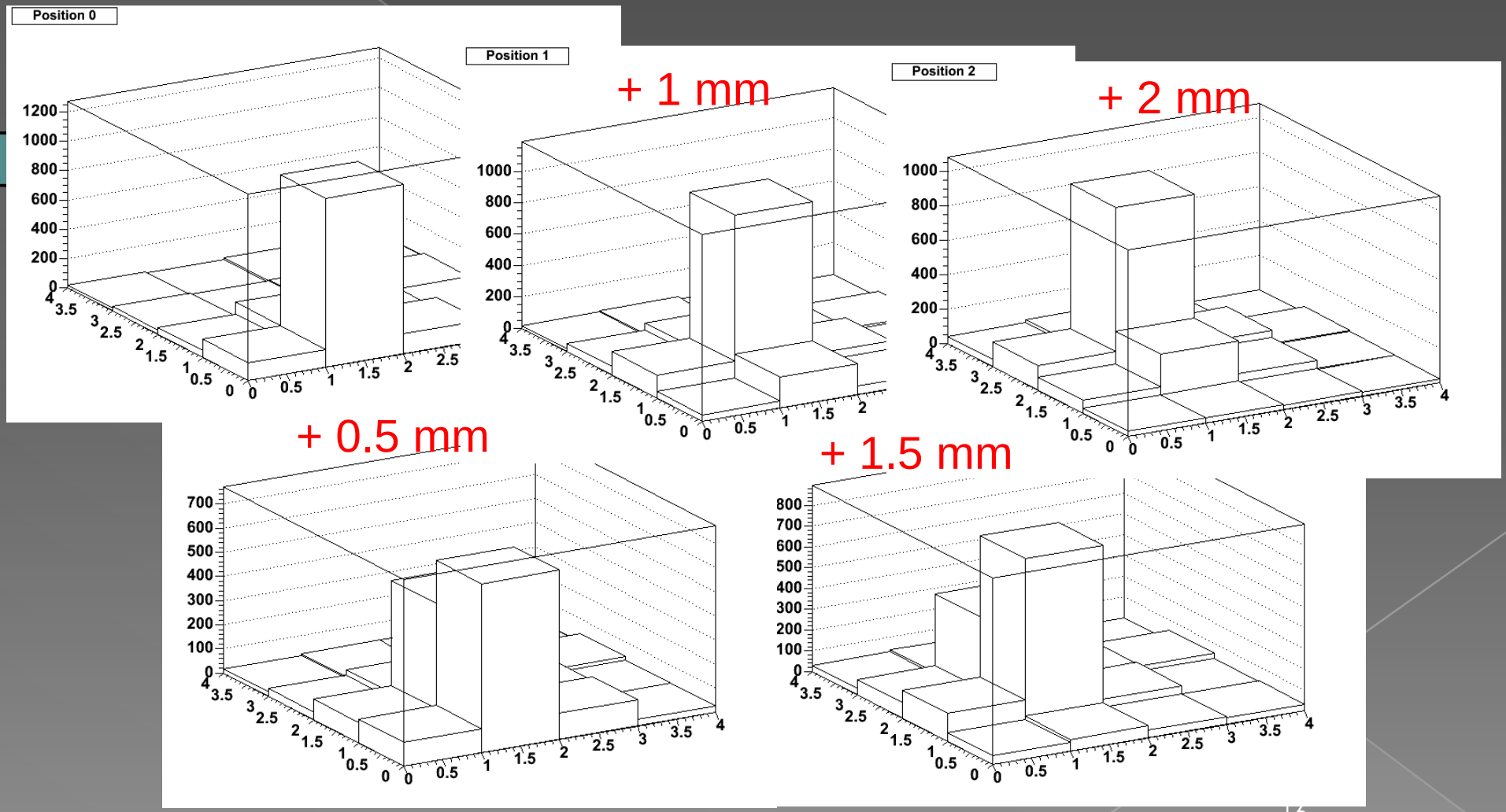

Position determination -black slab

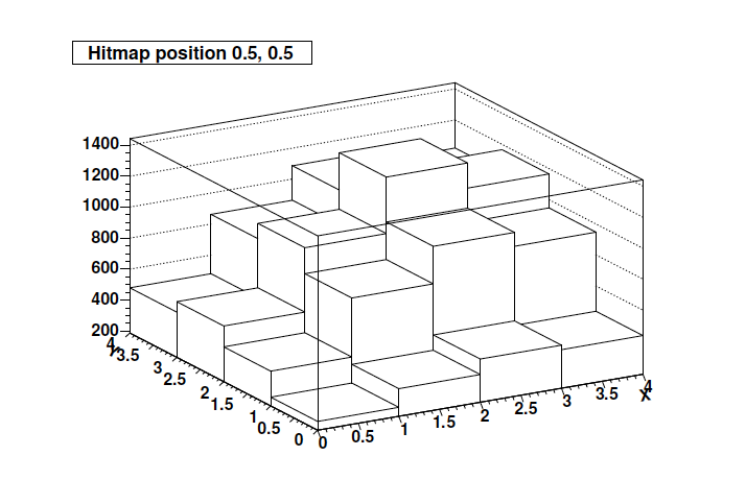

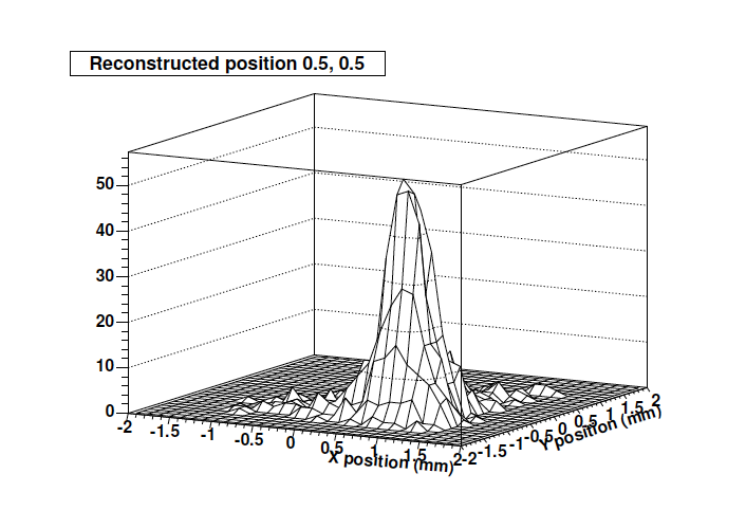

- Hitmap

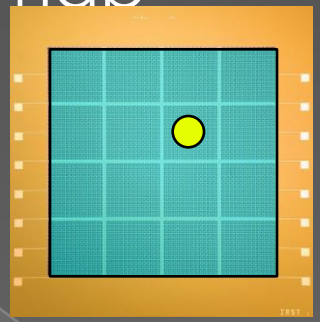

- "center of gravity" Algorithm

$$X = \frac{\sum X_i ADC_i}{\sum ADC_i},$$
$$Y = \frac{\sum Y_i ADC_i}{\sum ADC_i},$$

Position determination-black slab

- Matrix + LYSO crystal 4mm x 4mm x 5mm painted black
- Center of gravity algorithm – problems at the edges
- Difficulties due to the small size of the devices
- Intrinsic spatial resolution: 0.57 mm (FWHM) at CFOV

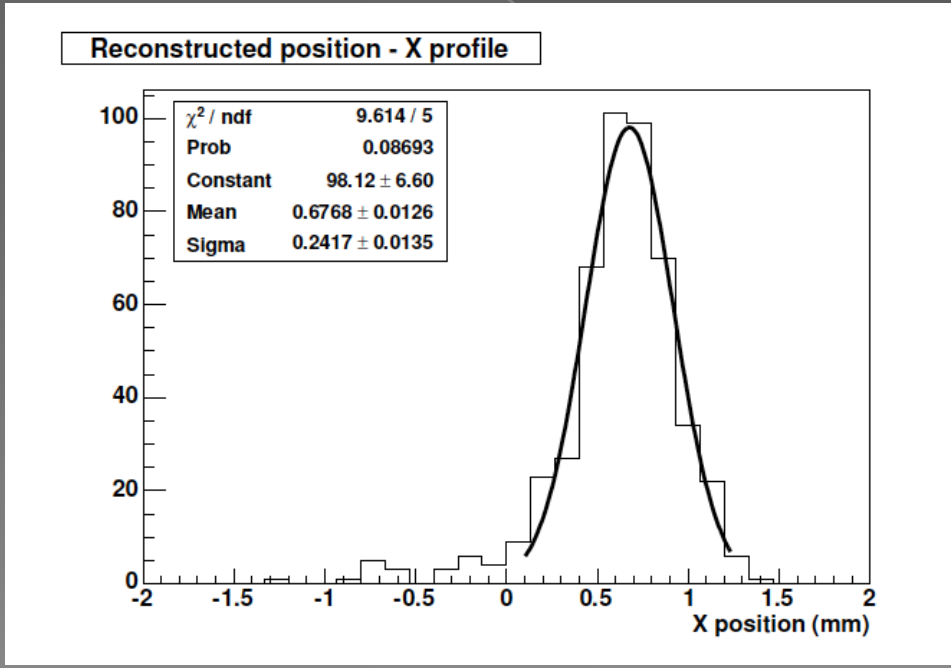

G.Llosa et al., Submitted to IEEE TNS, 2009

ge distortions

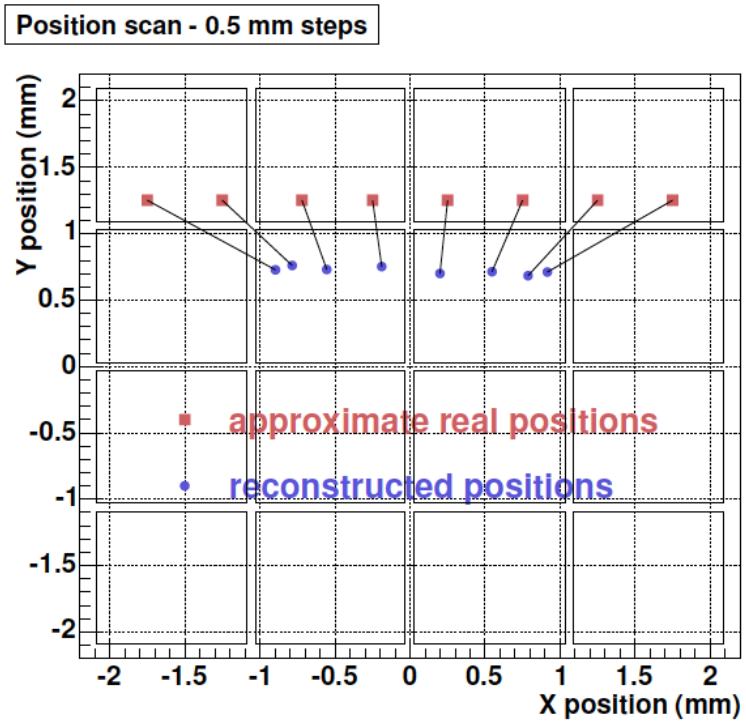

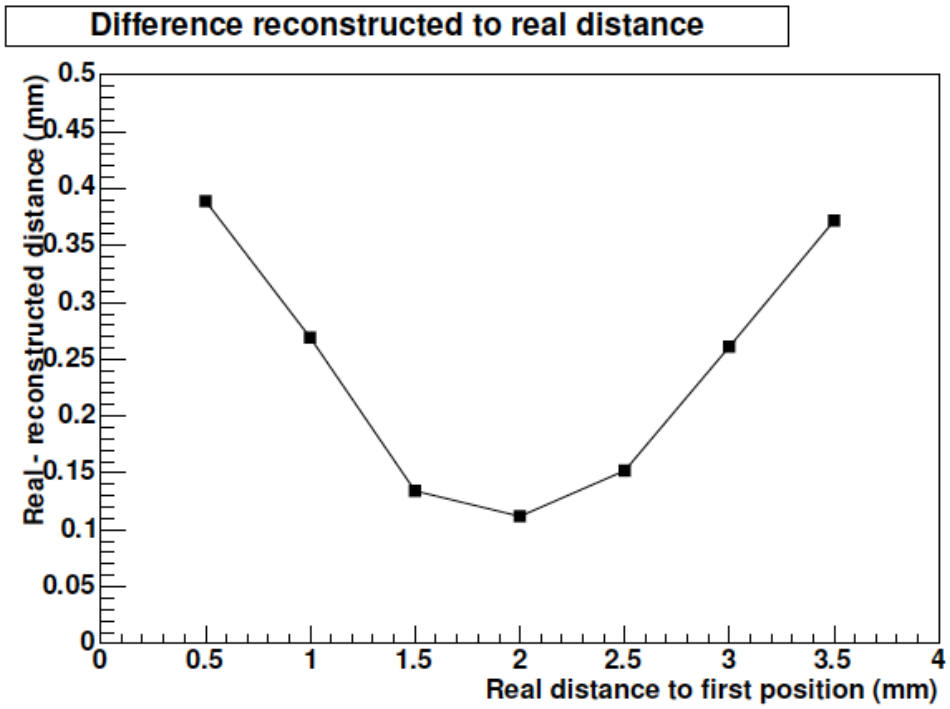

Results with continuous crystals

Crystal 4 mm x 4 mm x 5 mm covering the whole 4x4 matrix.

Na-22 spectrum summing signals from all channels.

$\Delta V_{over\text{-}br}$ =4V

$\Delta E/E$ =16%

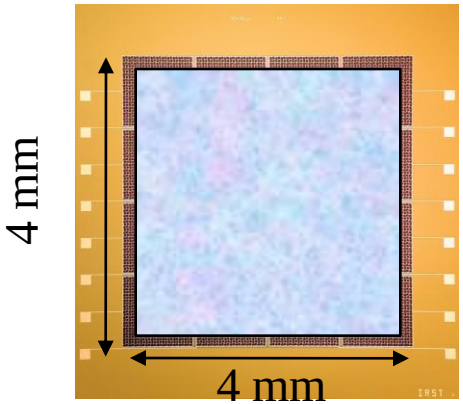

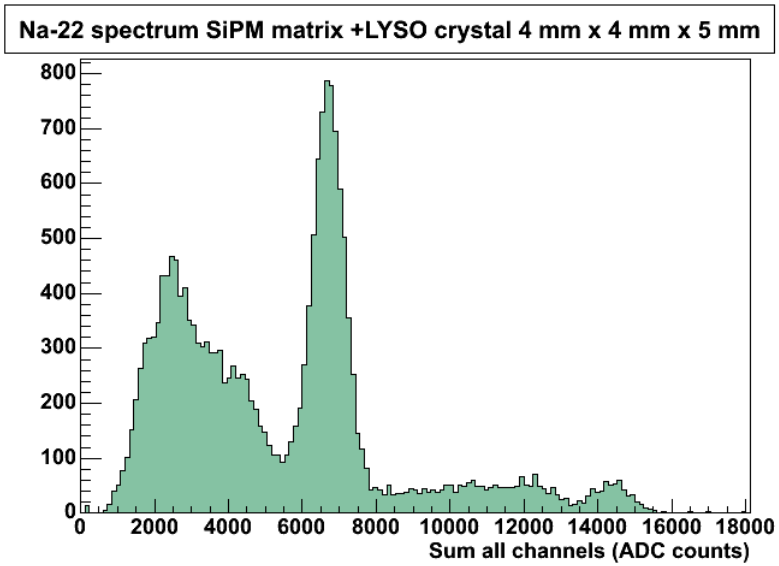

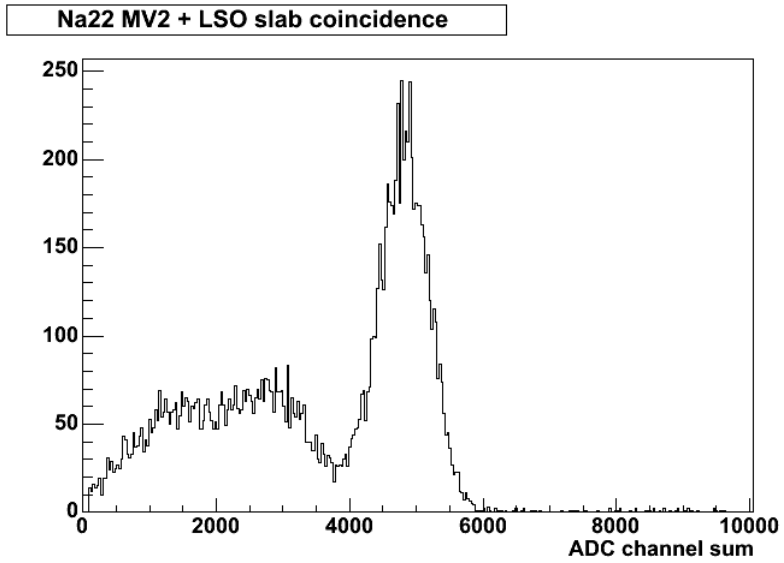

G.Llosa et al., Submitted to IEEE TNS, 2009

Matrices for INFN-DaSiPM2 project (2009)

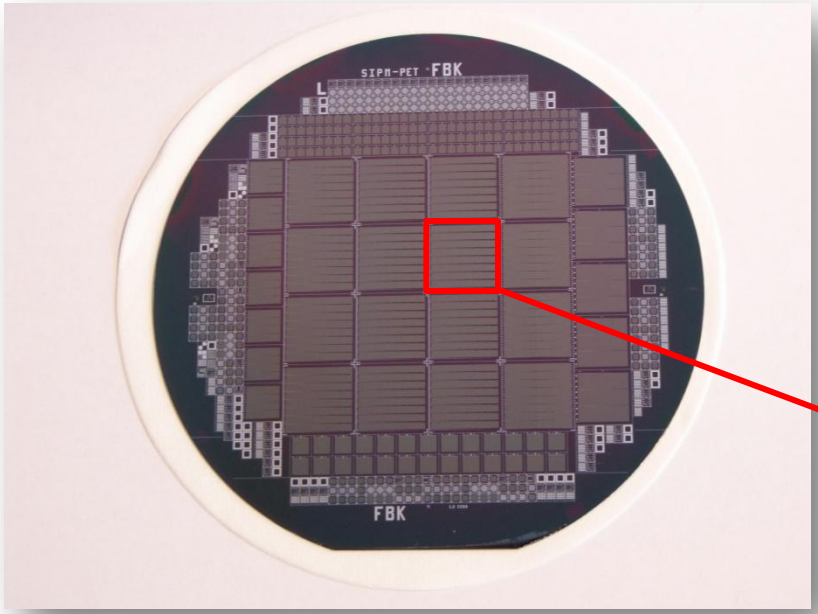

- 8x8 matrix
- 1.5mm element pitch
- 625 (50μm x 50μm) μcells
- read-out on one side

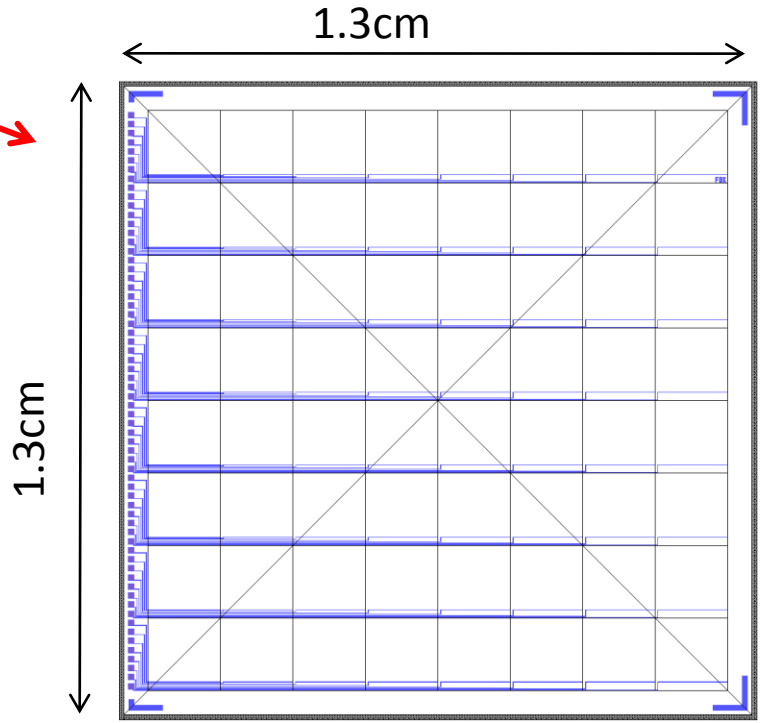

21

DaSiPM2 8x8 Matrices (2009)

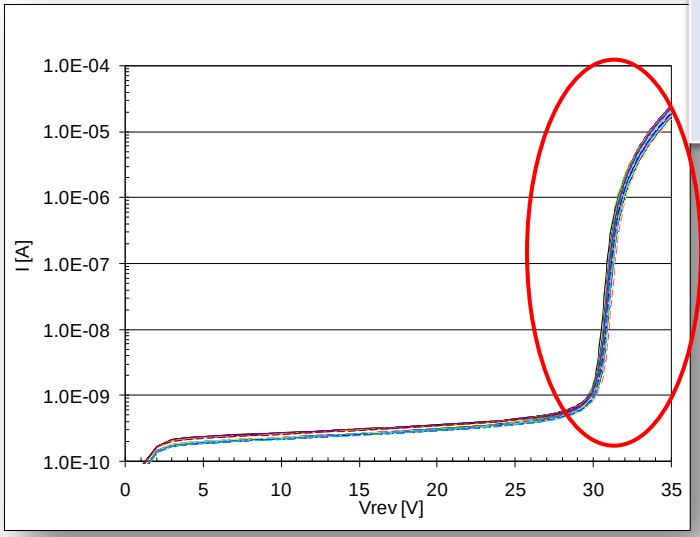

IV plot of the 64 elements of the matrix

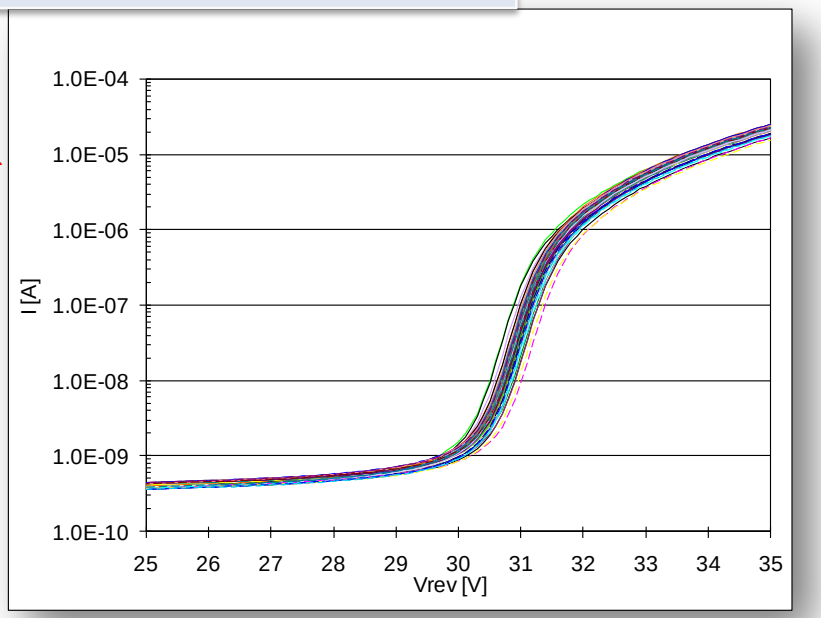

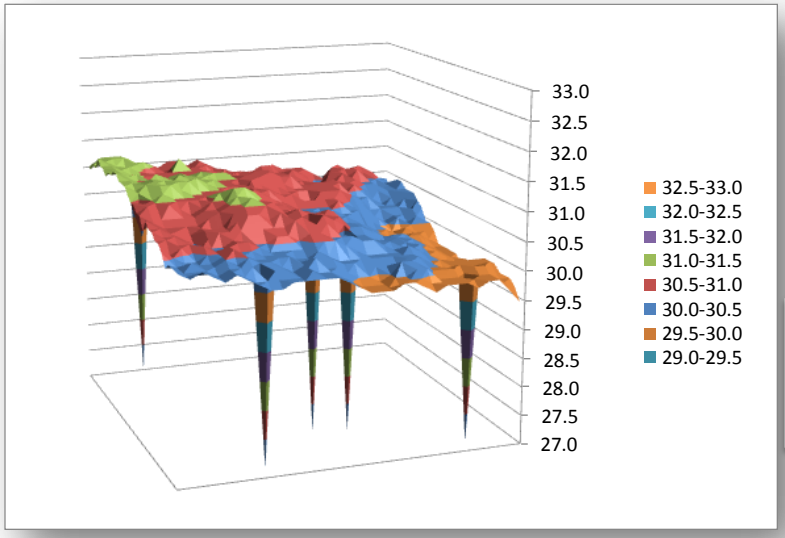

Breakdown voltage over the entire wafer surface

22

Matrix 8x8: first ^{22}Na spectrum

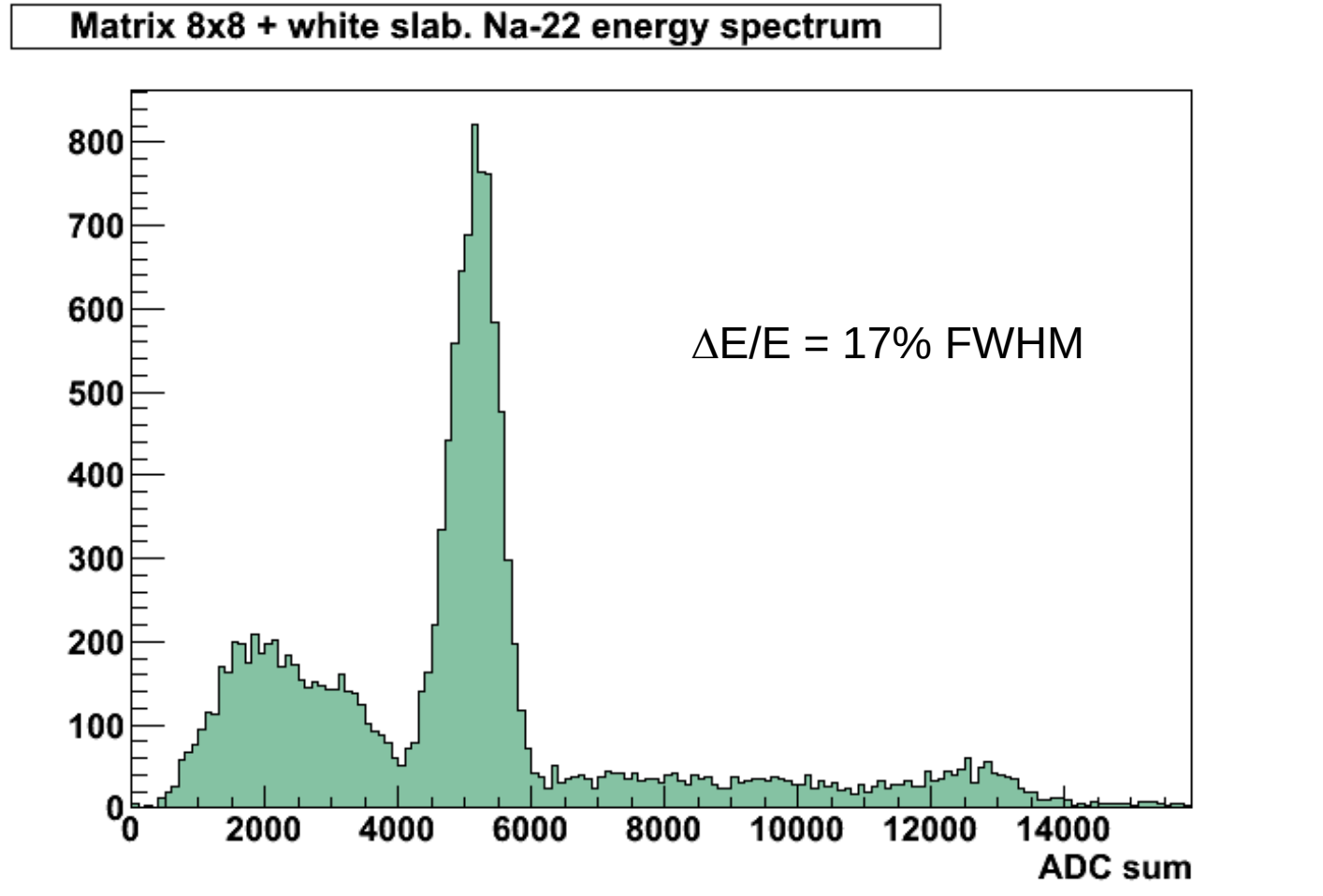

Preliminary data, April 2009, unpublished

PET/MR

PET-MR

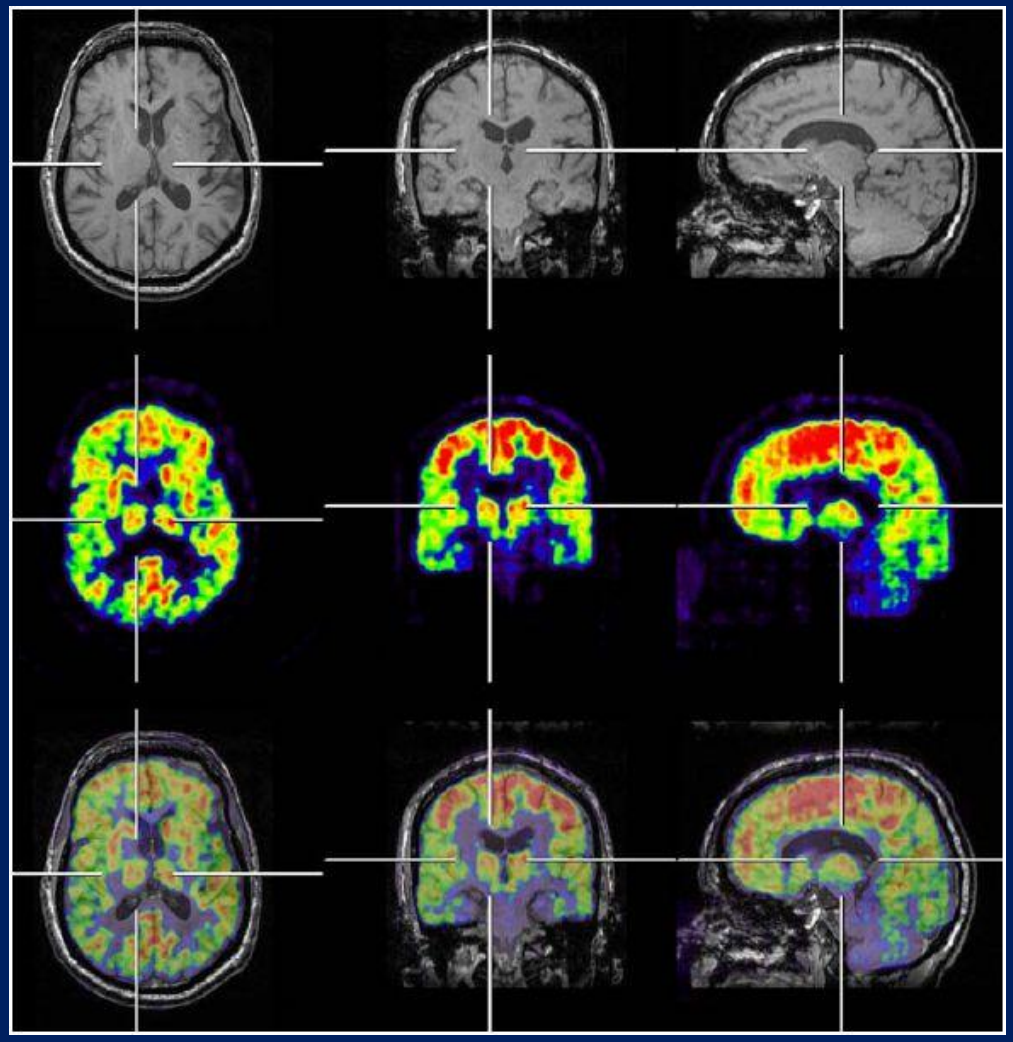

PET-MR

"PET/MR is a medical evolution based on a technical revolution"

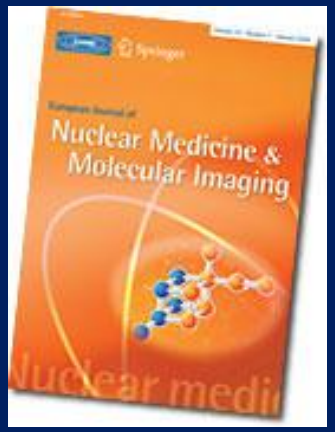

Volume 36, Supplement 1 / March, 2009
Multi-modality imaging: PET/MR

"We believe that both PET/CT and PET/MR are here to stay, because both platforms incorporate the diagnostic power of PET.
In fact, with PET/CT being a "dual-modality imaging" platform by virtue of combining functional (PET) and anatomical (CT) imaging, PET/MR offers true "multimodality imaging" by virtue of combining function (PET) and anatomy and function (both MR). This will open, without a doubt, new avenues in non-invasive imaging as part of clinical patient management and clinical research".

(T. Beyer and B. Pichler)

Technical Challenges in PET/MR

Interference on PET (photomultiplier and electronics)

- Static magnetic field
- Electromagnetic interference from RF and gradients

Interference on MR (homogeneity and gradients)

- Electromagnetic radiation from PET electronics
- Maintaining magnetic field homogeneity
- Eddy currents
- Susceptibility artifacts

General Challenges

- Space
- Environmental factors (temperature, vibration…)
- Cost

PET attenuation correction via MR data is a challenge!

PET/CT vs PET/MR

- Argument for integrated scanner won
- Increased patient throughput
- Enhanced diagnostic ability
  - fuse function and anatomy
- Same arguments and even more … apply to MR/PET

- A few examples of MR/PET

RAC + MR

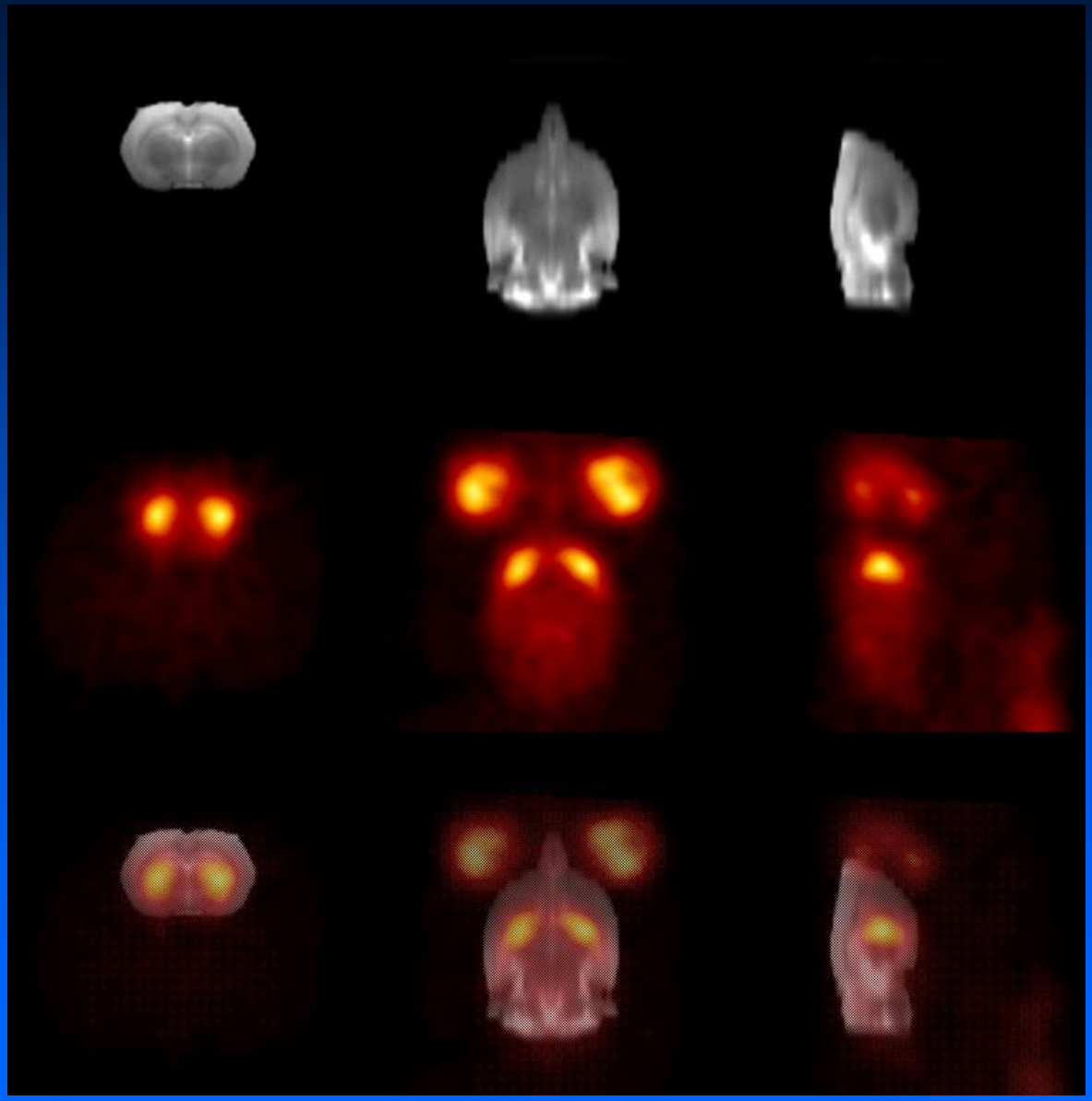

PET + MR: Semantic Dementia

MR

[^{18}F]FDG

Fused

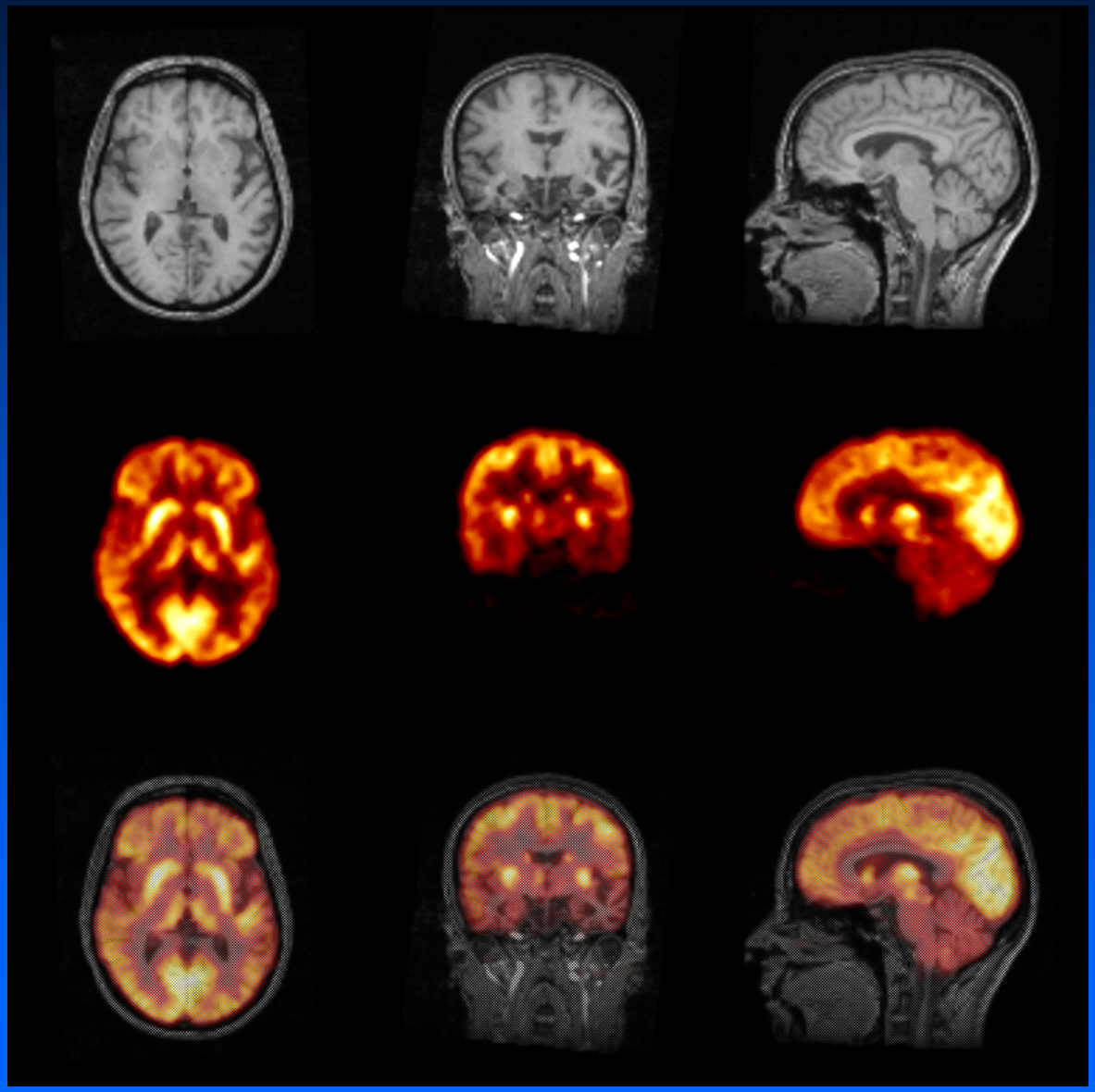

MR/PET:“one-stop-shop”

New whole-body imaging procedures allow comprehensive imaging examinations

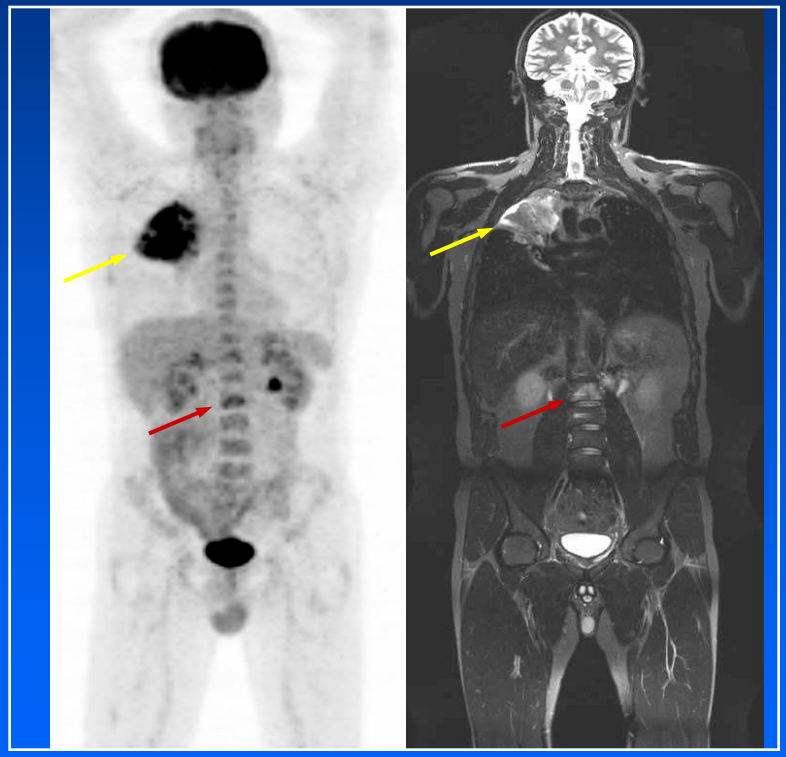

Coronal overview of 18F-FDG PET and MRI (T2- weighted Turbo-STIR)

Fused MRI/PET facilitates accurate registration of morphological and molecular aspects of diseases

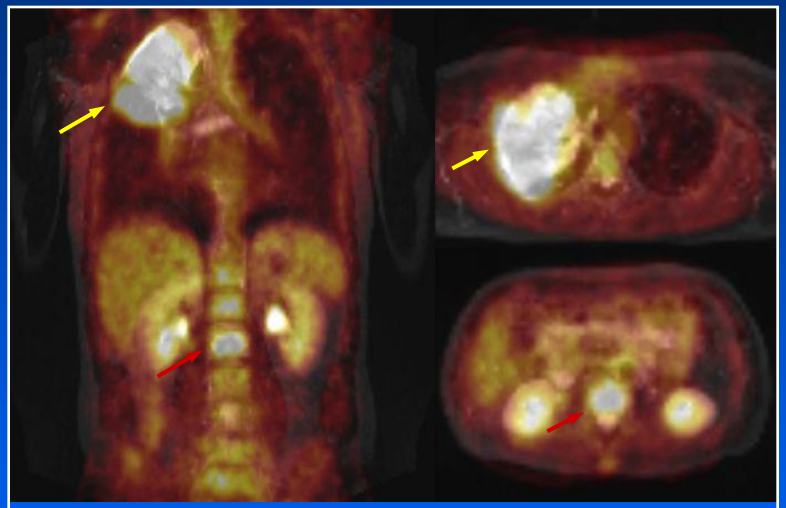

Pulmonary and osseous (arrow, red) metastatic disease of a non-small cell lung cancer (arrow, yellow)

Coronal and transversal MRI/PET fusion images

Courtesy of Dr. Gaa, TU Munich

Technology for MR/PET

- (1) Scintillating crystals plus photomultiplier tubes (PMT)
- (2) Scintillating crystals plus solid state light detectors

Technology for MR/PET (1)

- PMT Approach
  - Well understood, stable electronics, high gain (10^6)
  - However, Position sensitive PMT (PSPMT) operate in 1mT
  - Combination of distance (light guide) and iron shield (1-2mm of soft iron can further reduce 30mT -> 1mT) to operate in 1mT

Technology for MR/PET (1)

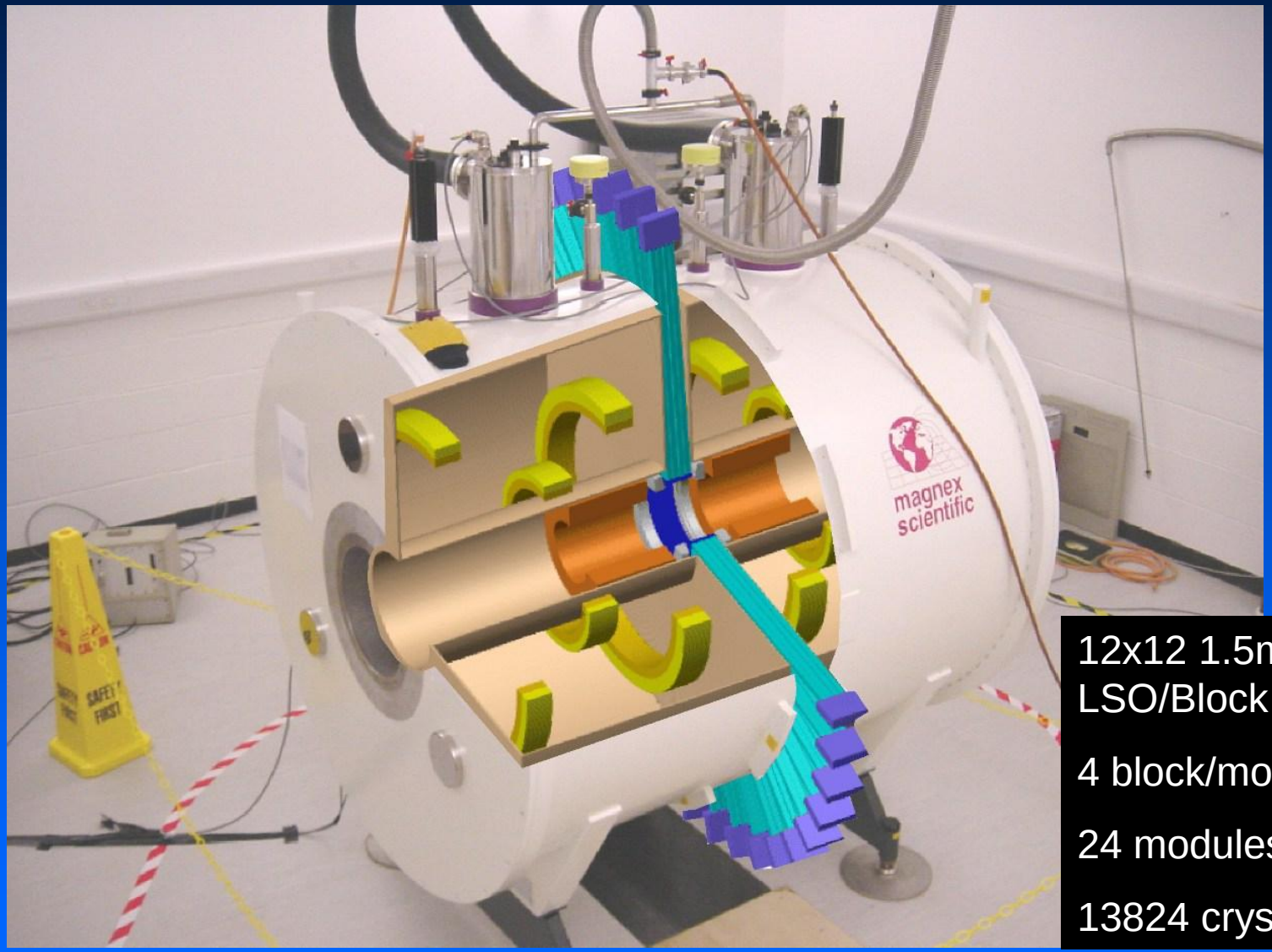

12x12 1.5mm LSO/Block

4 block/module

24 modules/ring

13824 crystals

Technology for MR/PET (1)

- 1mT has minimal effect on PSPMT performance
- Long light guides reduce energy resolution from 17 -> 27%, but this shouldn't have too big an impact upon performance
- Can perform simultaneous and isocentric MR/PET measurements
- However, small axial FOV

Technology for MR/PET (2)

- Solid state devices
  - Avalanche Photodiodes (gain ~ 150)
  - Silicon Photomultiplier (gain ~ 10^6)
  - Less well established as PET detectors
- Can operate in high static field > 7T
- Need to shield devices from both gradients and RF

Results: tests of SIPM in MR system (MRI)

in collaboration with the Wolfson Brain Imaging Center, Cambridge, UK

S.p.e and ^{22}Na energy spectra acquired with gradients off (black line) and on (red line).

No real difference is appreciated in the data.

Differences in photopeak position is due to temperature changes in the magnet (apparent change in gain due to changes in breakdown voltage).

Pickup in baseline when switching on/off

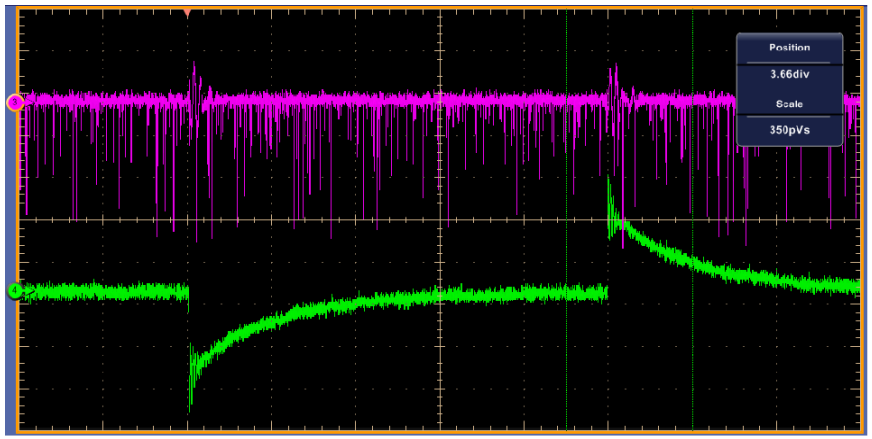

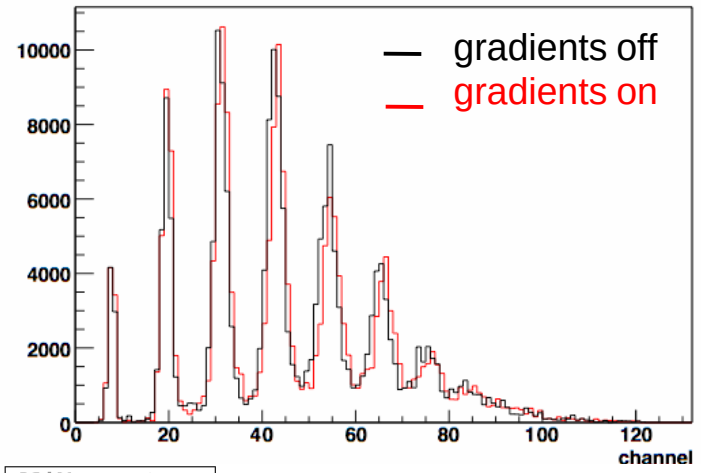

22^Na spectrum

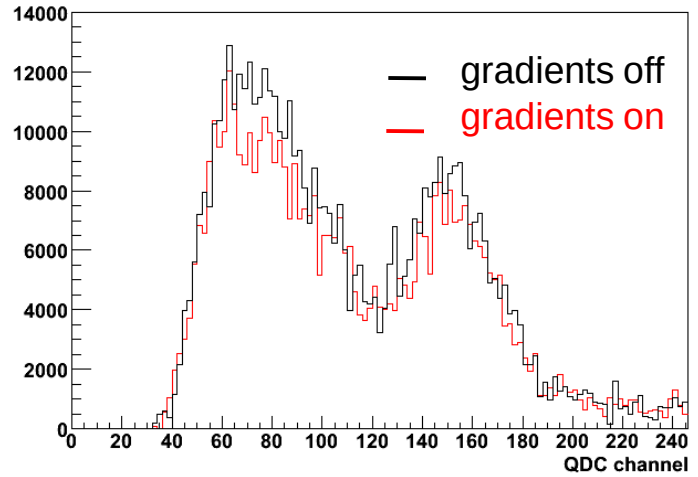

[R.C.Hawkes,et al. 2007 IEEE NSS-MIC, Honolulu, USA, October 28-November 3, 2007: M18-118.]

Brain PET/MRI

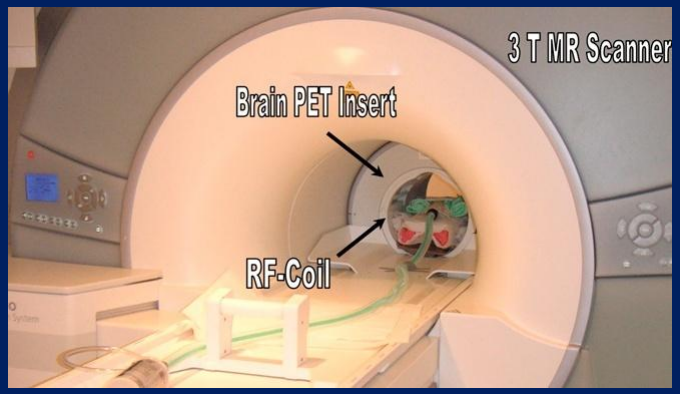

PET Insert

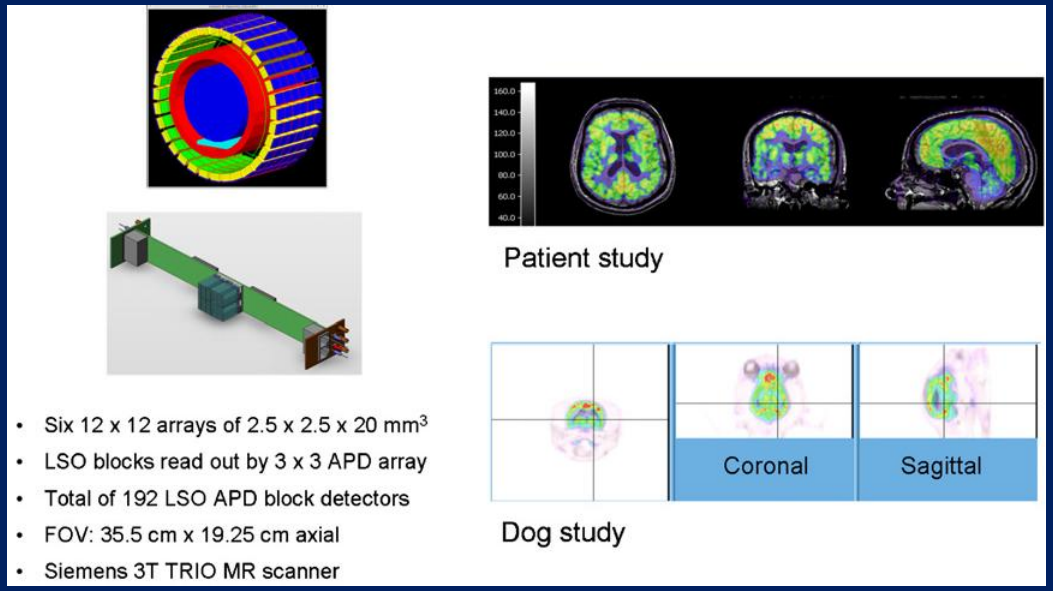

- Ring of LSO detectors inserted in a 3T MR tomograph
- Simultaneous PET and MR data acquisition

Courtesy of Berndt Pichler, University of Tübingen

MR/PET Head Insert

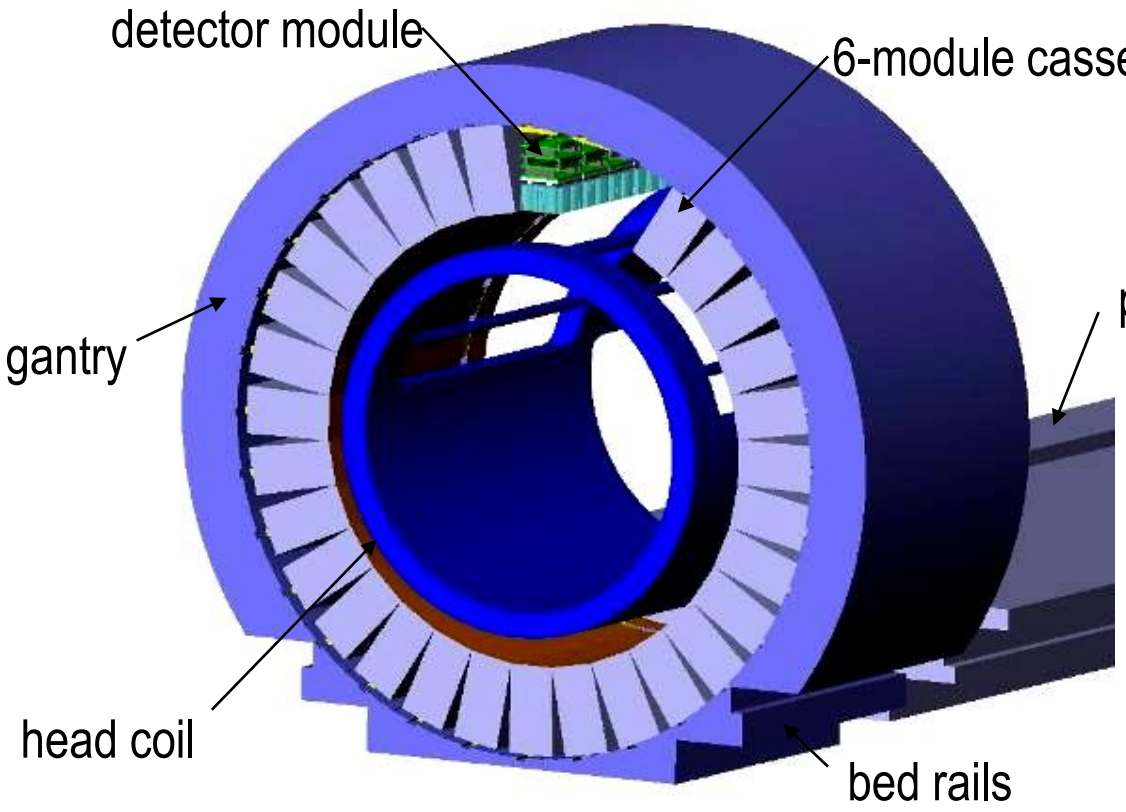

Scanner size: 36cm dia. x 20cm FOV

MR-PET Head Insert

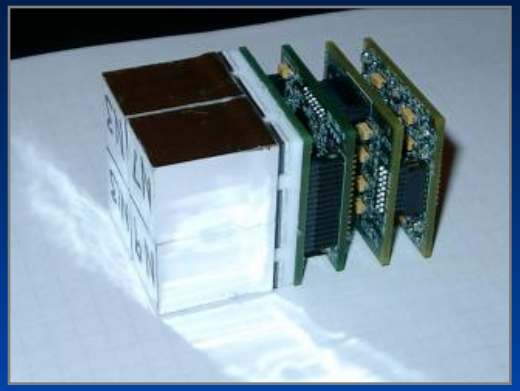

New integrated Detector Block

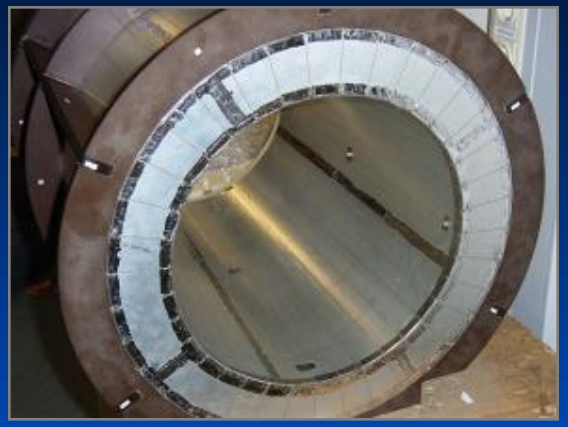

Prototype PET Head-Insert

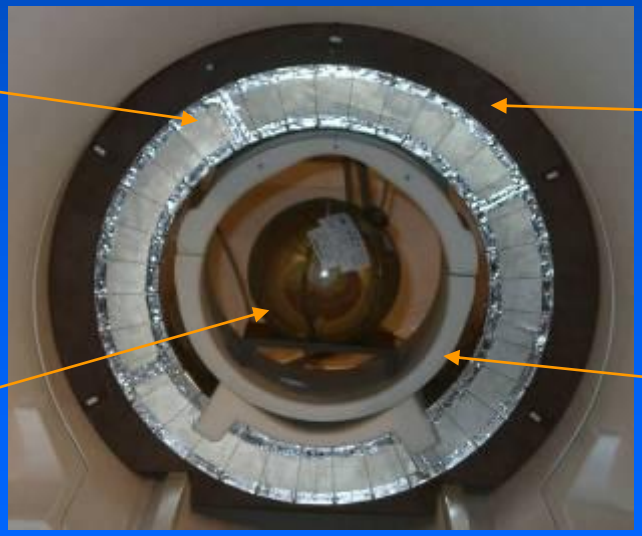

MR-PET Head Insert

- **Simultaneous dual-modality data acquisition**
  - **High resolution artifact free PET images**
  - **High resolution artifact free MR images**

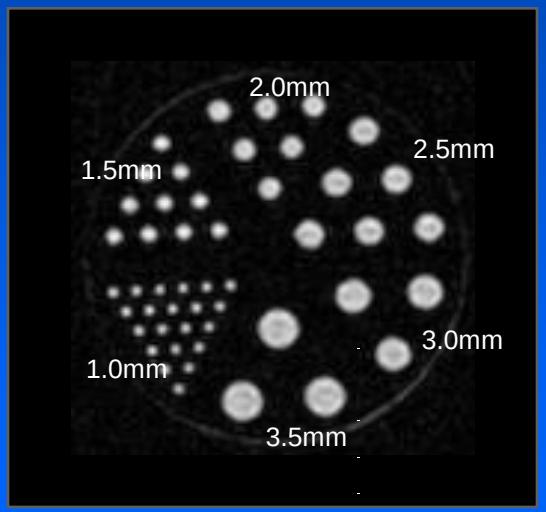

MR

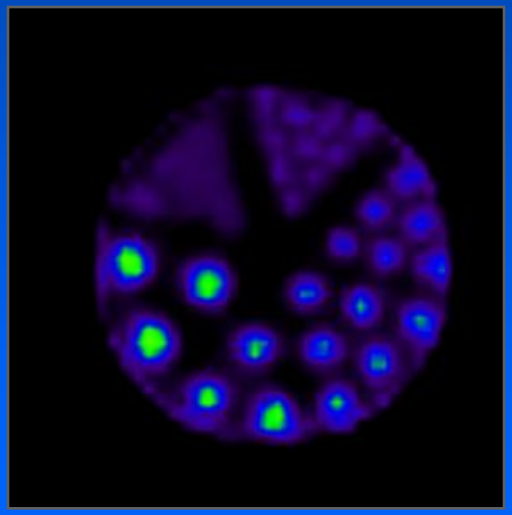

PET

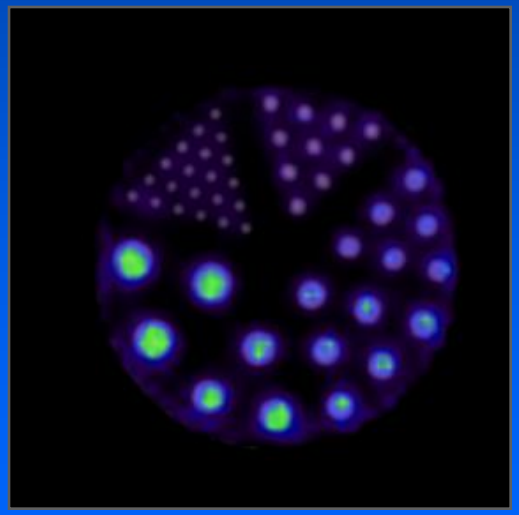

MR-PET

Wholebody MR/PET

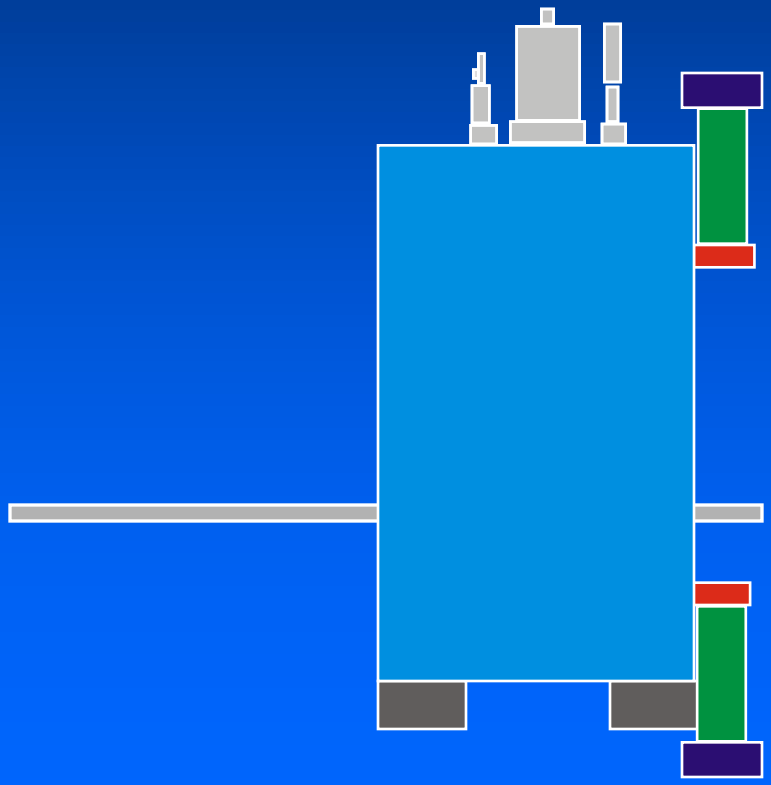

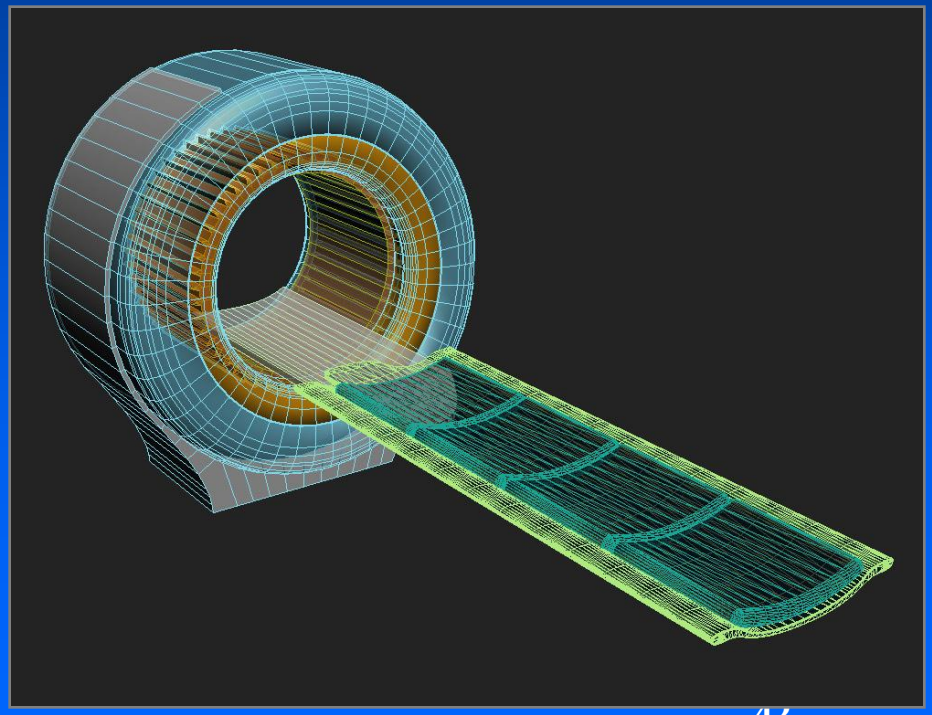

PET on-line in Hadrontherapy

Combatting Cancer with Radiotherapy

GOAL➔ Achieving a higher dose deposition to the tumor regions still sparing surrounding healthy tissues.

FROM X-RAYS TO HADRON THERAPY
WHAT ARE THE EXPECTATIONS?

- **Favorably shaped energy deposition curve;**
- **Negligible lateral spreading;**
- **High LET radiation just before coming to rest.**

WHAT IS THE CLINICAL IMPACT?

Hadron Therapy
Physical advantages of hadron beams

exponential attenuation
vs
Bragg peak

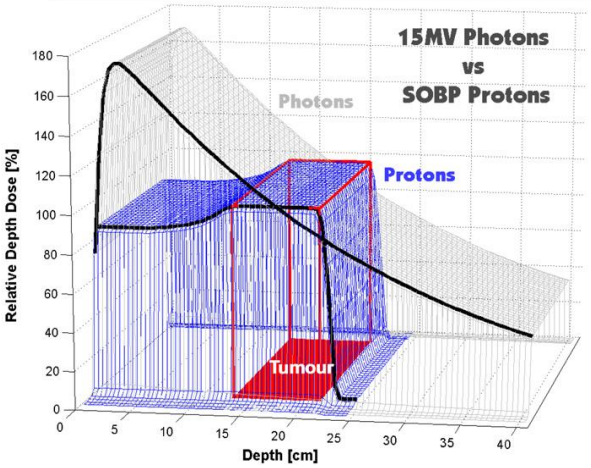

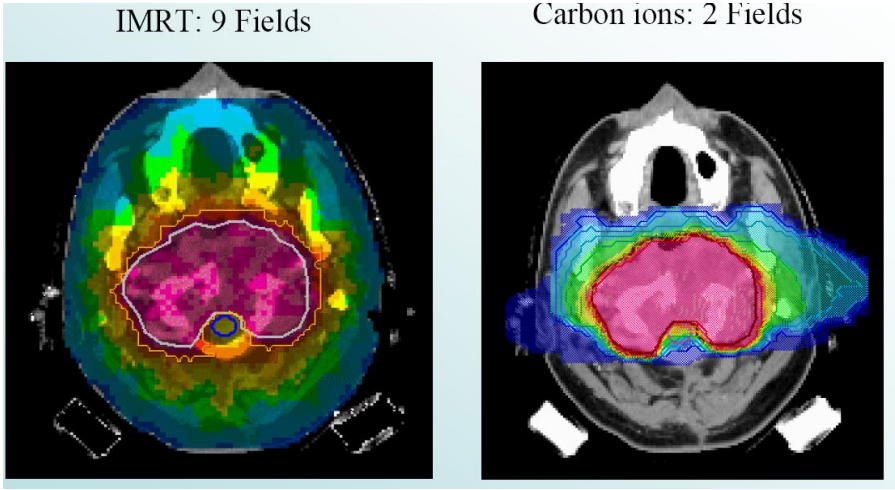

M Kraemer and M Scholz, 2000, Treatment planning for heavy ion therapy
Phys. Med. Biol. 45 3319–30

- **Increase of conformity and reduction of integral dose**
- **Improve local control rate**
- **Higher survival rate.**

Hadron Therapy
Biological advantages of high LET radiations

Compared to X-rays:

- **Higher RBE (Relative Biological Effectiveness):**
  - **lower repair of irradiation damages**;
- **Smaller differences between cell cycle phases:**
  - **growing and dormant tumor cells killed**;
- **Lower OER (Oxygen Enhancement Ratio):**
  - **good and bad blooded tumor regions killed**;
- **Lower fractionation effect:**
  - **lower damage of normal tissue;**
  - **lower necessity of repair capacity**.

Hadron Therapy
Why we should think to something more

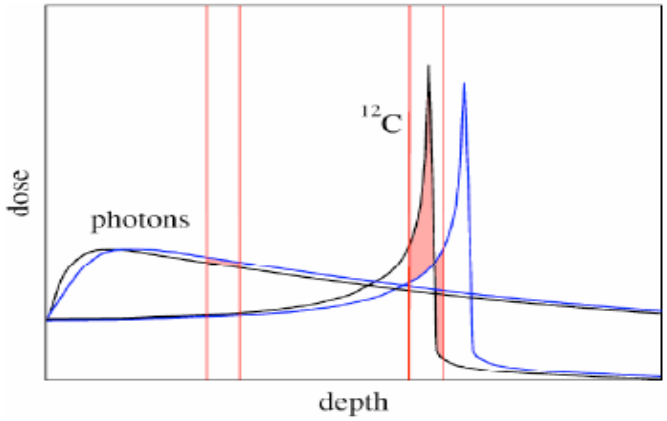

High gradients in the dose profile make the clinical practice require a highly precise superposition of such gradients on tumor boundaries.

•ARISING DIFFICULTIES:

- **Approximations of dose calculation methods**

- **Differences between treatment preparation and treatment delivery**
  - Possibilities of patient misalignment;
  - Anatomical or physiological variations among different treatment sessions;
  - Internal organ motion.

The principle of PET monitoring

- **Positron Emission Tomography (PET) is potentially a unique tool for *in vivo*, *non invasive* monitoring of the precision of the treatment in hadrontherapy.**
- **Therapeutic hadron beams produce in the biological tissues short - lived β^+ emitters by means of projectile and/or target nuclei fragmentations.**

isotope ^{A}X	half life $T_{\frac{1}{2}}$ [s]	β^+ spectrum endpoint [MeV]
^{11}C	1222.8	0.96
^{15}O	122.2	1.73
^{10}C	19.3	0.90
^{13}N	597.6	1.19

- Nuclear cross sections fall off at low energy just few millimeters before Bragg peak.

- Finding the distribution of positron annihilation points it would be possible to extract non invasively **in vivo information about dose localization**.

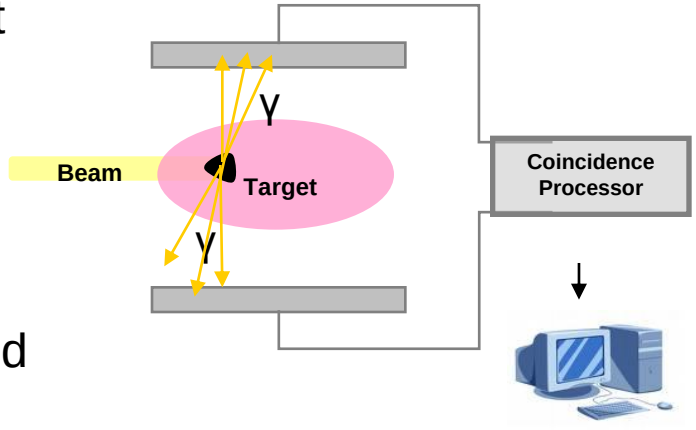

The principle of PET monitoring

- **The case of light ions irradiation: e.g. protons, He,..**

Low - Z beam ($Z \leq 6$):

$\mapsto$ Target β^+ activation

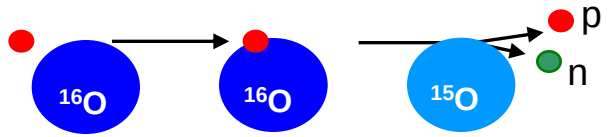

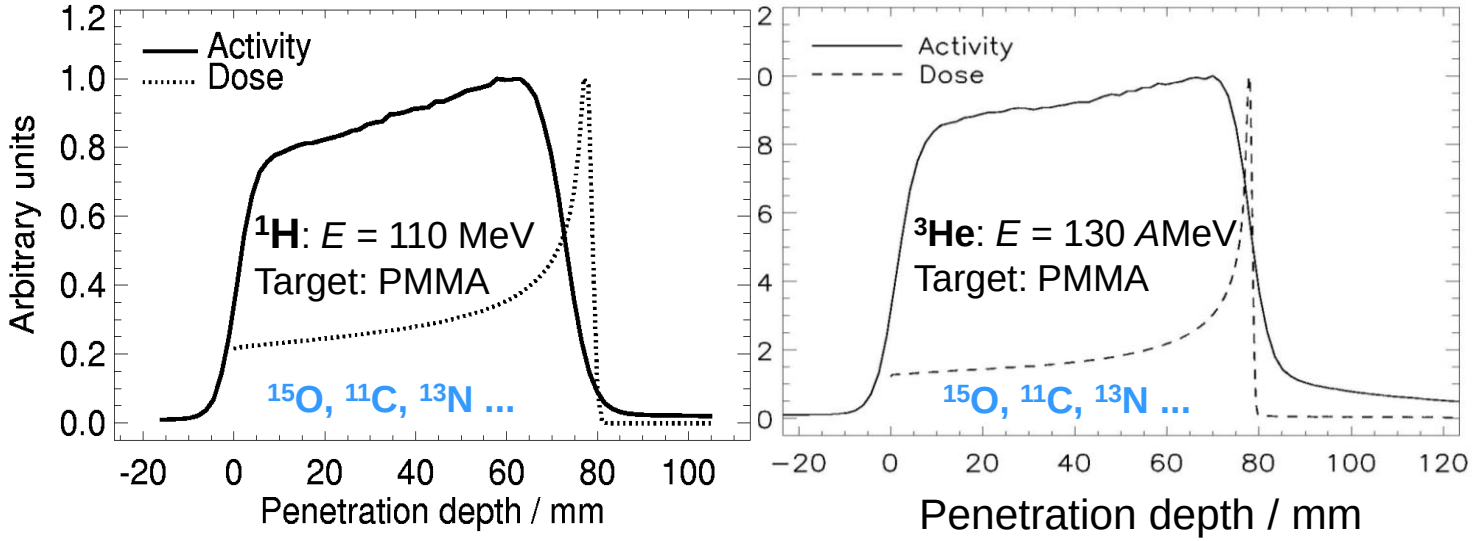

J Pawelke et al., Proceeding: Ion Beams in Biology and Medicine (IBIBAM), 26.-29.09.2007, Heidelberg, Germany

The principle of PET monitoring

- **Light ions versus heavy ions:**

High - Z beam ($Z \geq 6$) :

$\mapsto$ Target β^+ activation

$\mapsto$ Projectile β^+ activation

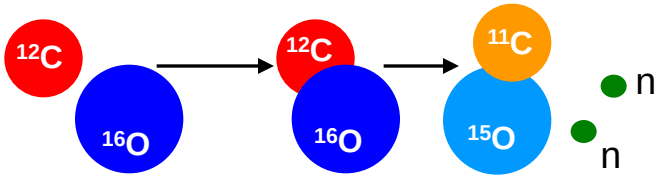

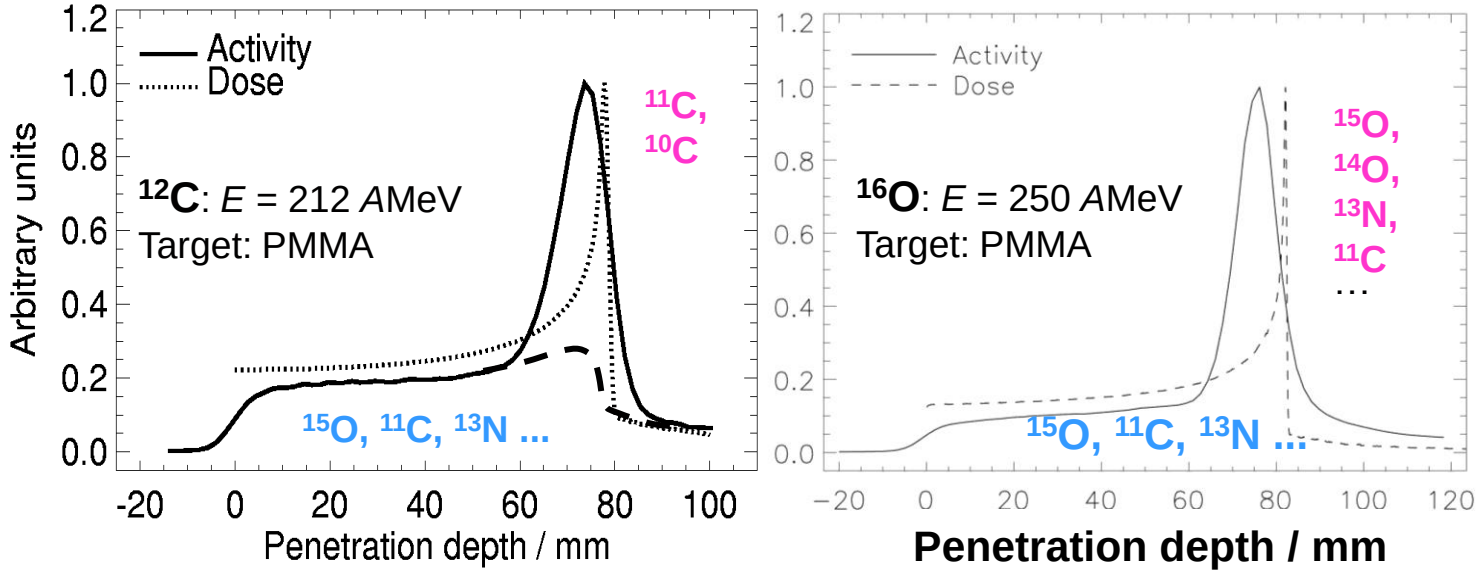

J Pawelke et al., Proceeding: Ion Beams in Biology and Medicine (IBIBAM), 26.-29.09.2007, Heidelberg, Germany

Towards the final GOAL:
The Unfolding Procedure

The correlation between dose and activity profiles must be extracted in order to derive from the measurements the information of dose distribution and to compare it with the planned one :

$$D_{Inferred}(z) \quad \Leftrightarrow \quad D_{TPS}(z)$$

But we measure the activity that is not linearly related to the dose:

$$A(z) \neq D(z)$$

It requires a strategy for range verification:

- **Choice#1:**

Ideal approach for MC dose quantification on the basis of PET images:

- Implement a MC program which automatically produces the most probable activity distribution corresponding to the activity distribution measured via PET
- MC, that produces the most probable activity distribution, also gives the most probable dose
- However, MC is still too much time consuming and not proven yet in clinical➔ TPS are based on analytical models

Towards the final GOAL:
The Unfolding Procedure

❖ Choice#2: Filtering approach*

$$A_{Measured}(z) = f(z) \cdot D_{Inferred}(z)$$

$$\Downarrow$$

$$D_{Inferred}(z) = f^{-1}(z) \cdot A_{Measured}(z)$$

Exp #1. Phantom study at Catana (LNS, Catania, Italy)**

$$D_{Diode\ Measured}(z) \cdot f(z) = A_{Inferred}(z)$$

$$\Updownarrow$$

$$A_{Measured}(z)$$

Exp #2. Patient study at MGH (Boston, USA) ***

$$D_{TPS}(z) \cdot f(z) = A_{Inferred}(z)$$

$$\Updownarrow \quad \Leftrightarrow A_{\text{Measured}}\ (\text{still to be done})$$

$$A_{MC}(z)$$

* Parodi K and Bortfeld T, Phys. Med. Biol. 51 (2006) 1991 - 2009.

**Attanasi et al., Phys Medica 24(2) (2008) 102-6.

***Attanasi et al., to be submitted to Phys Med Biol (2009).

The experience from in-beam PET phantom experiments @ CATANA with proton beams

Centro di AdroTerapia e Applicazioni Nucleari Avanzate (LNS, Catania,IT)

SC cyclotron - based facility for ocular melanomas treatment.

The CATANA facility
The Beam Delivery System

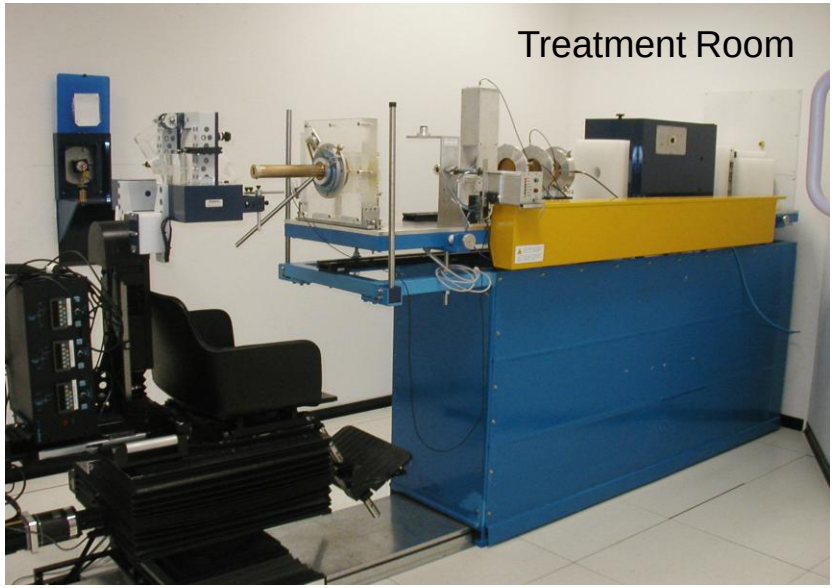

The Beam Line @ Catana

- E_max: 62 MeV protons;
- Fluence: 10^6-10^8 particles/s;
- Passive beam shaping:
  - range shifters and
  - modulator wheels;
- Final collimator: max 25 mm.

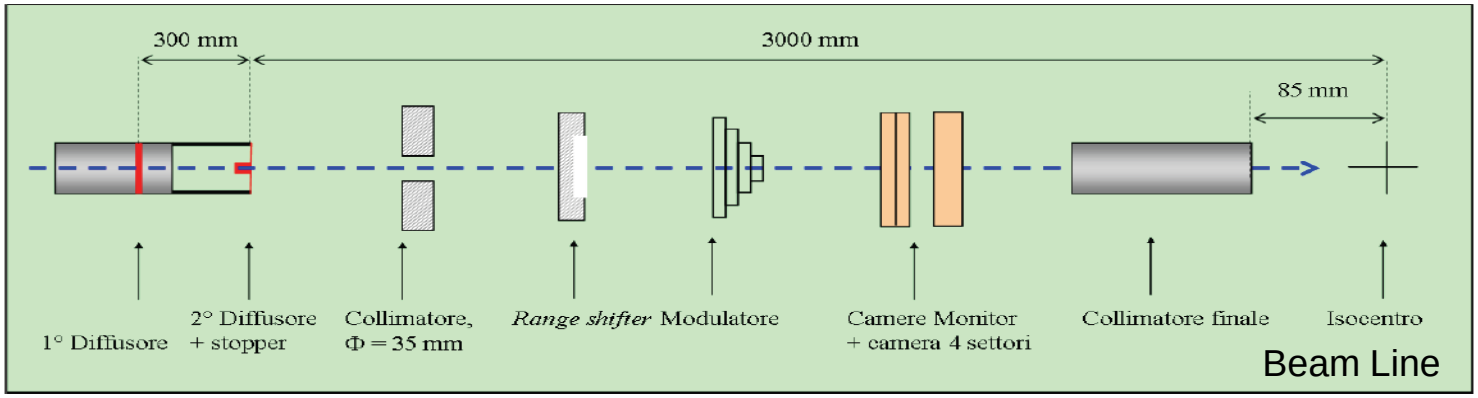

Exp#1: The DoPET project (INFN) (Dosimetry Positron Emission Tomography)

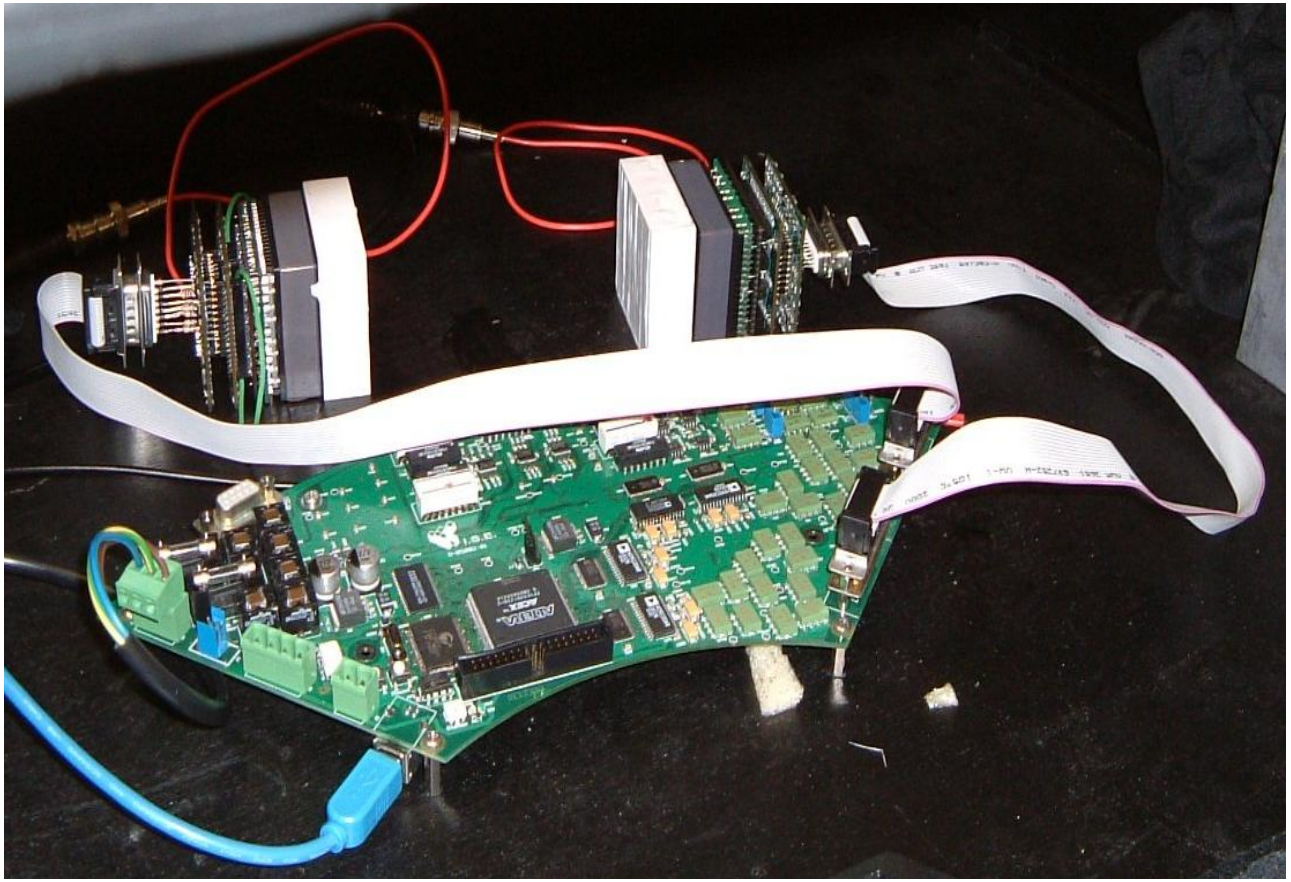

Dedicated “home-made” PET prototype

The Tomograph Architecture
Detector head

- **Scintillating crystals LYSO:Ce** from Hilger Crystals Ltd:
  - 21 x 21 pixels;
  - 2 x 2 x 18 mm^3 pixel dimensions.

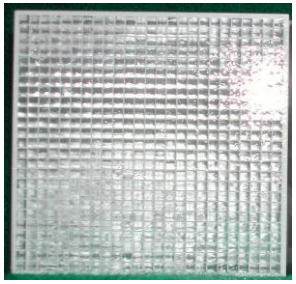

- **PS-PMT H8500** from Hamamatsu Photonics K.K.:
  - 49 x 49 mm^2 active area, 8 x 8 anodes;
  - 12 stage dynode.

- **Front-end electronics**:
  - Resistive chain 64 inputs/8+8 outputs SCD (symmetric charge division);
  - 2D chain 8+8 inputs/2+2 outputs;
  - pre-amp (PSP).

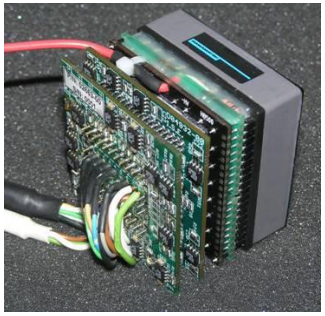

The experiments on homogeneous phantoms
Irradiation & Imaging

- Homogeneous cylindrical phantoms of PMMA at center of FoV;
- Spread-out Bragg Peak irradiation (SOBP, 10.8 mm plateau width);
- Delivered dose: 30 Gy;
- Irradiation Time: 20-60 s;

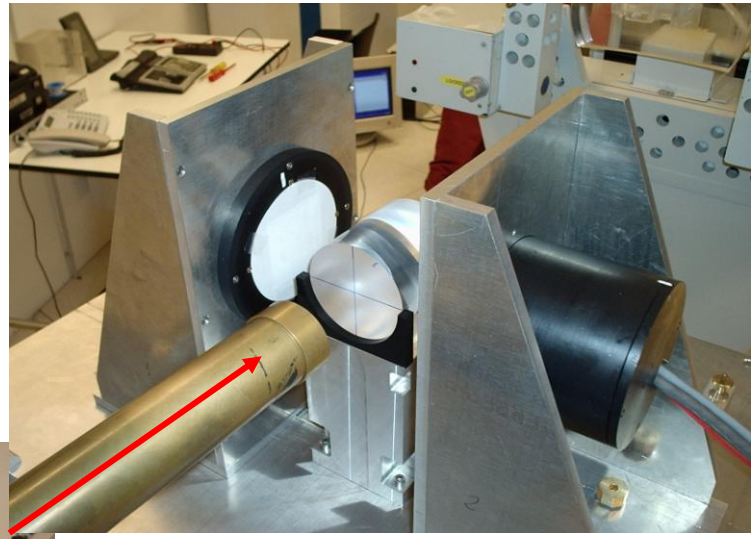

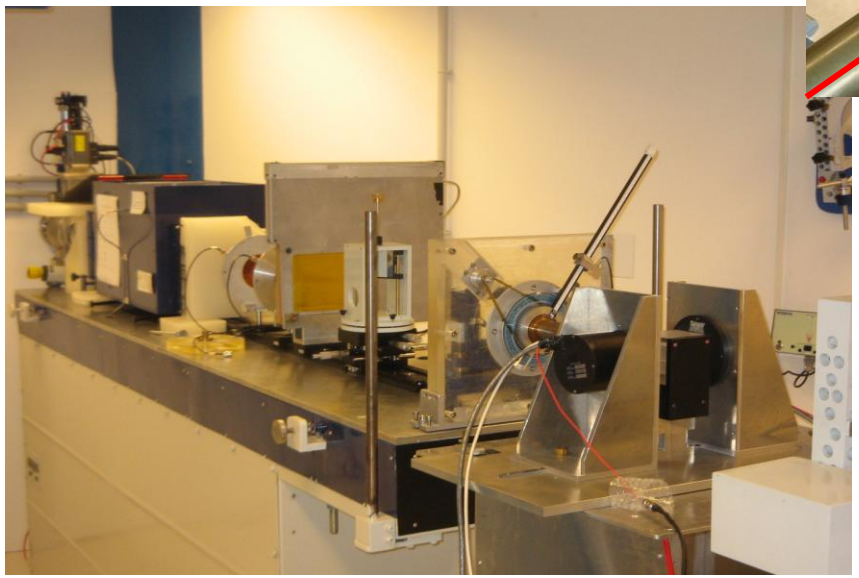

- Final collimator: 25 mm Ø;
- Distance between detectors:14 cm.
- PET acquisition time:20 min.
- FoV: 42 x 42 x 42 voxels.
- 1.076 x 1.076 x 1.076 voxel dimension.

The experiments on homogeneous phantoms
The feasibility of range monitoring

- **SOBPs irradiation of PMMA phantoms** were performed using different range shifters along the beam line so that each irradiation differed from the other ones only in the proton range, *with variations less than 2 mm*.

Range shifters

Label	Material	Equivalent thickness in PMMA (mm)
a2	Aluminum	1.9
a3	PMMA	2.9
a4	PMMA	3.9
a6	PMMA	5.8

- Preliminary dosimetric measurement of each selected dose configuration was performed for accurate irradiation planning.

The experiments on homogeneous phantoms

The feasibility of range monitoring

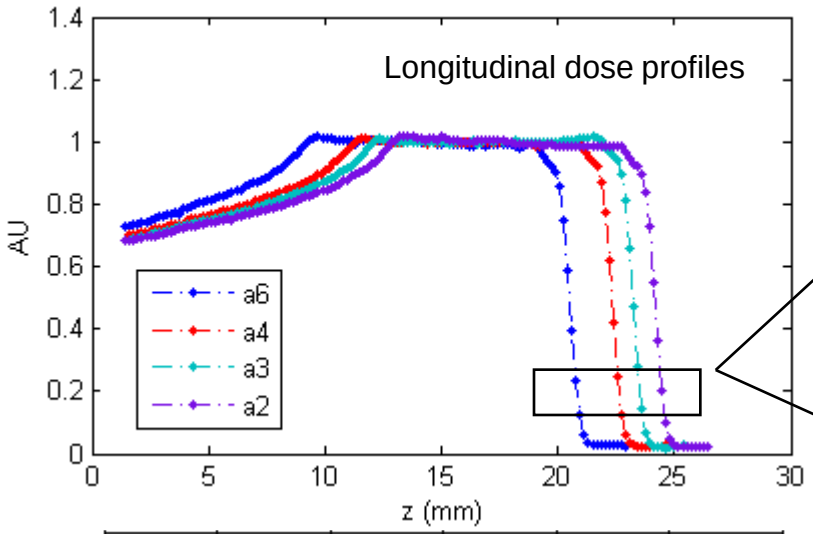

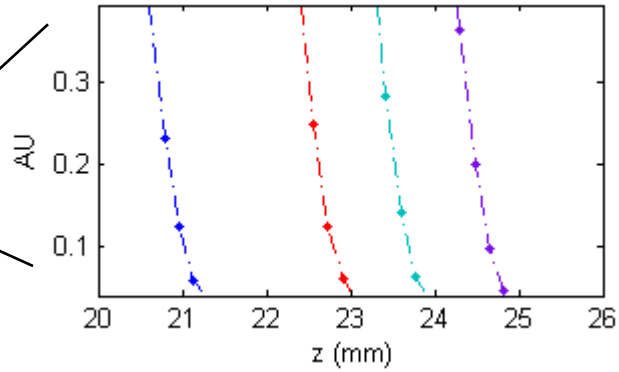

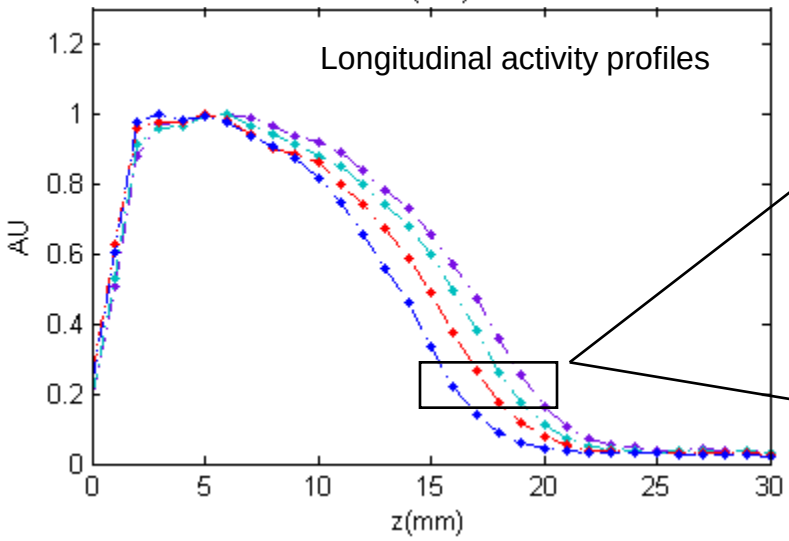

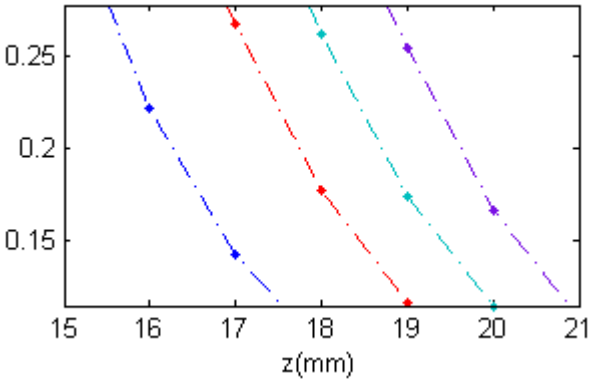

- Vecchio, S. et al, ", IEEE Trans Nucl Sci 2009, 56(1), 51-56.
- F. Attanasi et al., Nuclear Instruments and Methods in Physics Research A 591 (2008), 296–299

The experiments on homogeneous phantoms
Reproducibility of range measurement

Extended irradiation of PMMA phantoms and data acquisition were repeated five times under nearly identical experimental condition.

- *Aims:*
  - Study of the variability in the reconstructed activity;
  - ***Estimate of the accuracy*** on 50% position of the distal activity distribution for proton range monitoring.

- *Method:*
  - Variance analysis.

The experiments on homogeneous phantoms
Reproducibility of range measurement

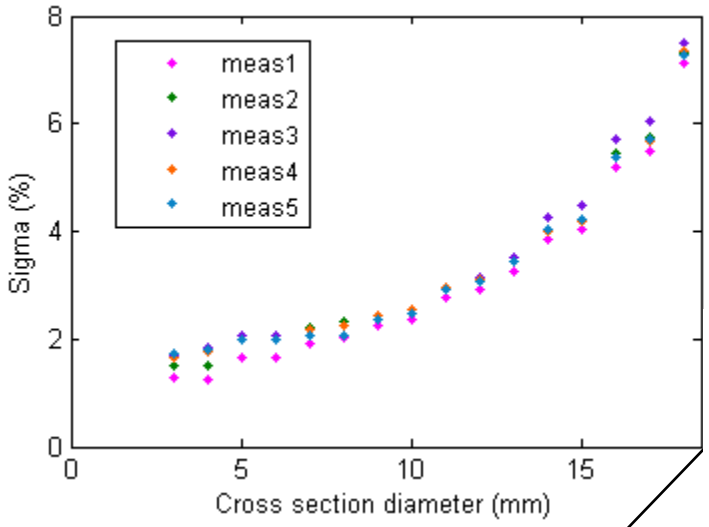

Variability in the reconstructed activities increases considering larger volumes around the beam central axis. It doesn't take more than **~3%** in the subvolume with a cross section diameter of 10 mm.

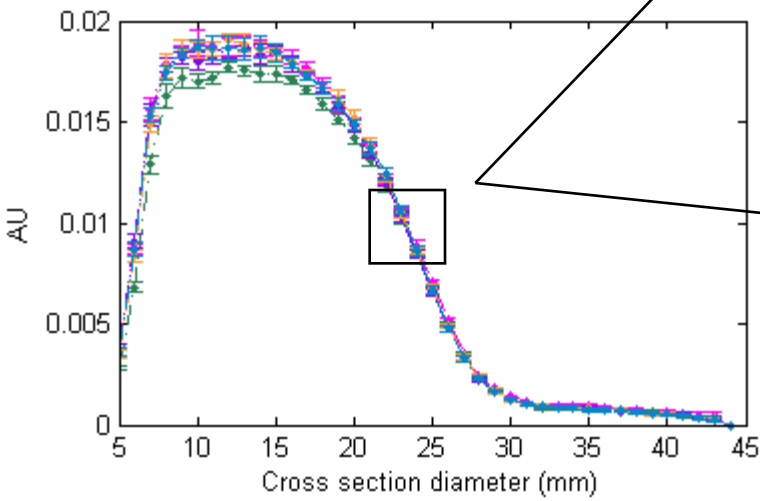

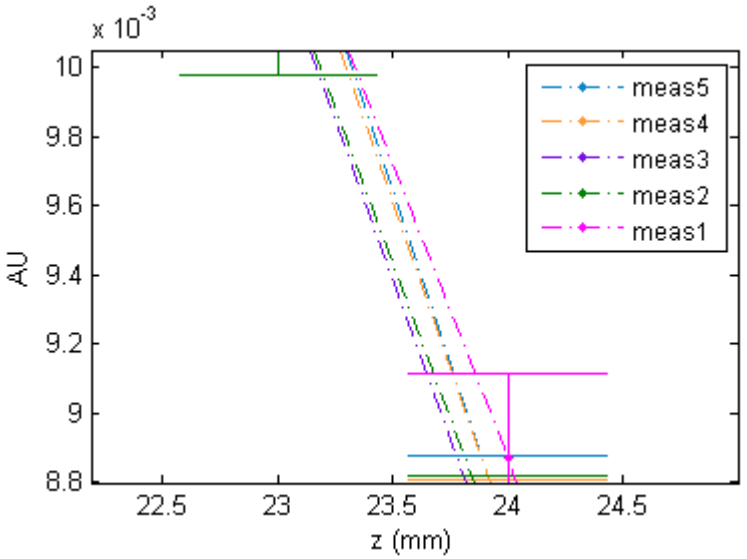

50% fall off activity distribution is reproduced with an accuracy of about **± 200µm**

Resolution of air gaps in PMMA phantoms within the irradiation field

PMMA phantom with 0.5 cm Air_Gap at 2 cm depth;

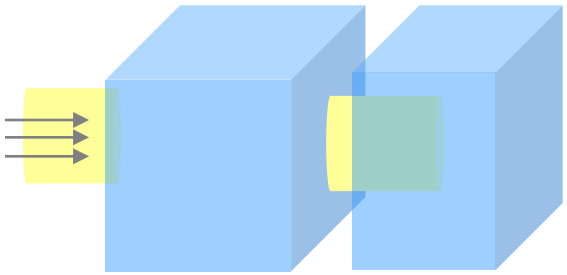

- **Phantom irradiation:**
  - **Bragg peak dose: 30 Gy**
  - **Irradiation time: 18 s;**
- **Beam cross section: 2.5 cm Ø;**
- **Acquisition time: 20 minutes**

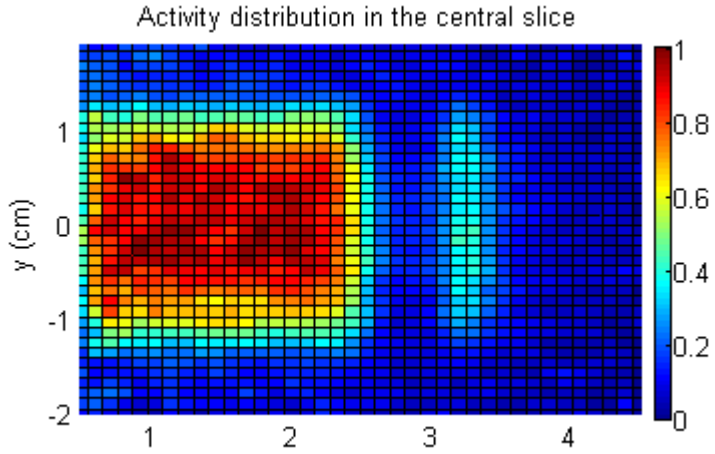

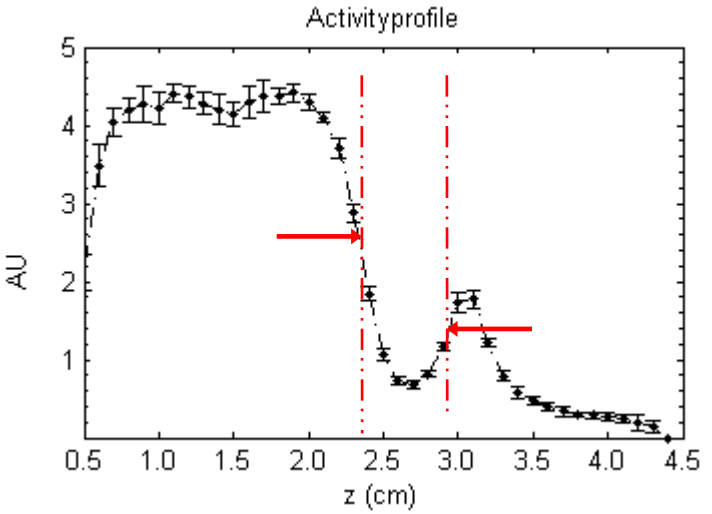

Resolution of air gaps in PMMA phantoms within the irradiation field

•**Three holes collimator: 0.5 cm Ø each**;

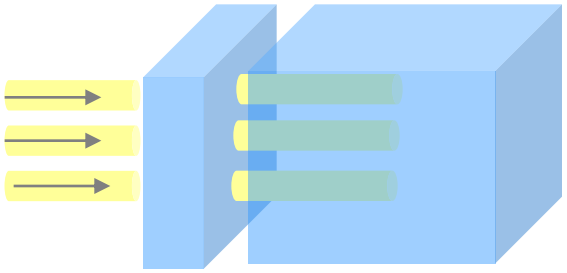

PMMA AIR PMMA
0.5 0.2 3 cm

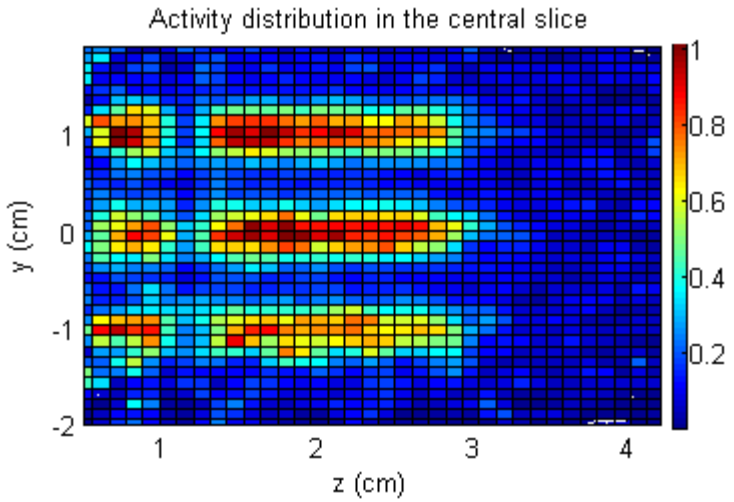

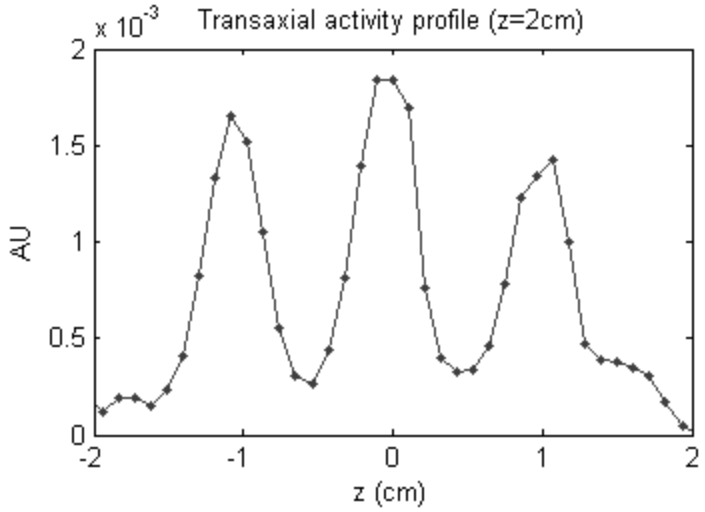

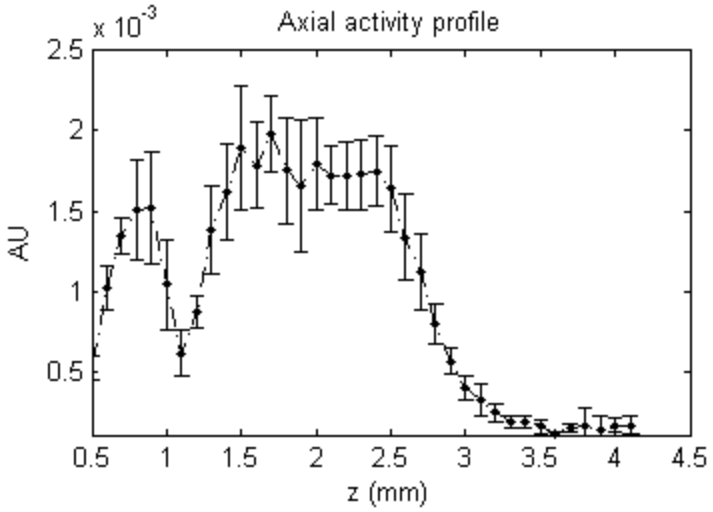

The experiments on slab phantoms
Sensitivity of the PET method

- Materials

	ρ (gr/cm³)	H(%)	C(%)	O(%)	Ca(%)	N(%)
PE	0.94	14	86	--	--	--
PMMA	1.18	8.05	59.99	31.96	--	--
BONE	1.819	3.41	31.41	36.50	26.81	1.84

- **Time analysis on the measured data**
  - **The separation of isotope contributions**

$$\forall\ (\text{subset, voxel}):$$

$$n_{[t_i,t_{i+1}]}(x,y,z) = \sum_j N_j^{T_{Irr}}(x,y,z)\cdot\left(e^{-\frac{t_i}{\tau_j}} - e^{-\frac{t_{i+1}}{\tau_j}}\right)$$

$$\text{with}\quad N_j^{T_{Irr}} = N_j^{Tot}\,\frac{\tau_j}{T_{Irr}}\left(1-e^{-\frac{T_{Irr}}{\tau_j}}\right)$$

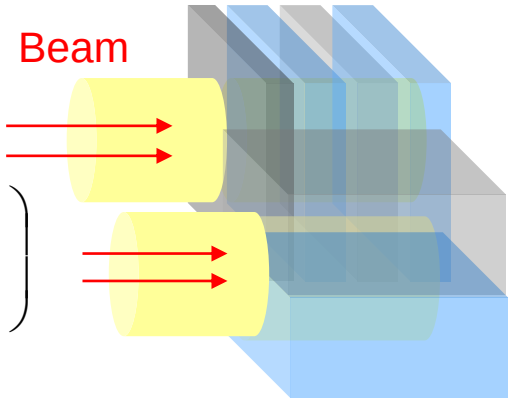

The experiments on slab phantoms
Sensitivity of the PET method

PE/PMMA slabs phantom

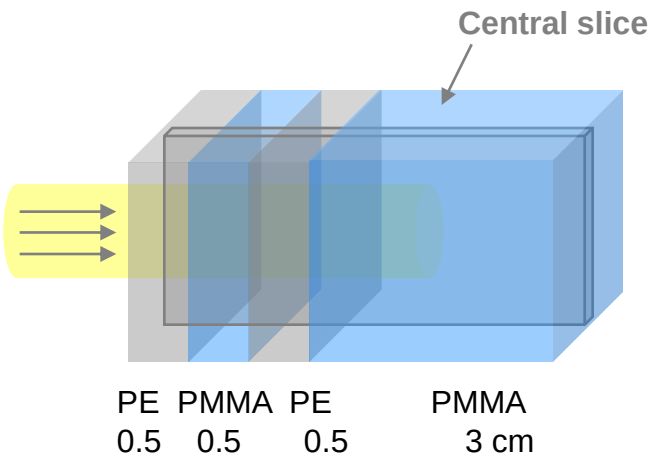

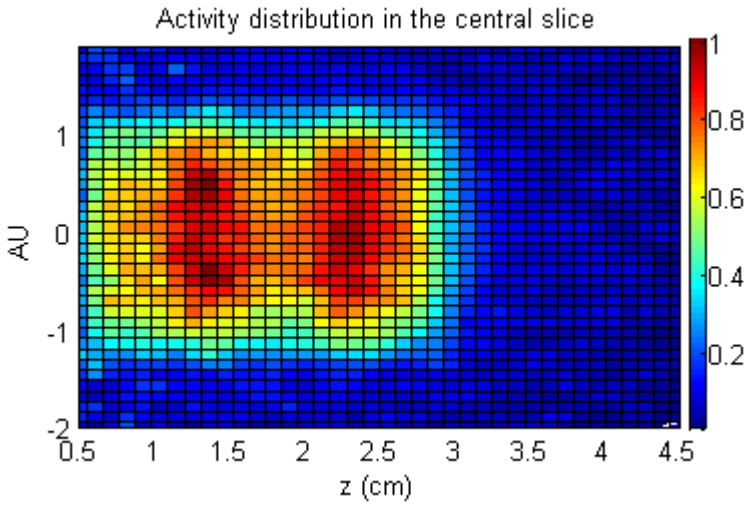

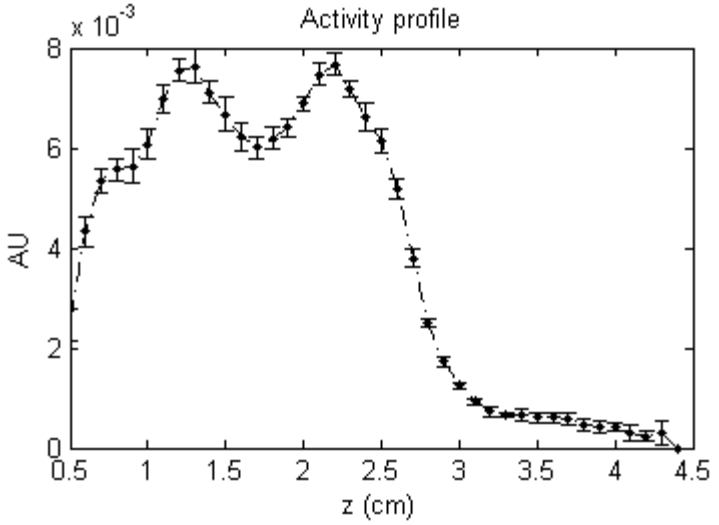

- **Monoenergetic irradiation:**
  - **Bragg peak dose: 30 Gy**
  - **Irradiation time: 18 s;**
- **Beam cross section: 2.5 cm Ø;**
- **Acquisition time: 20 minutes;**

The experiments on slab phantoms
Sensitivity of the PET method

Reconstructed isotope distributions in the central slice

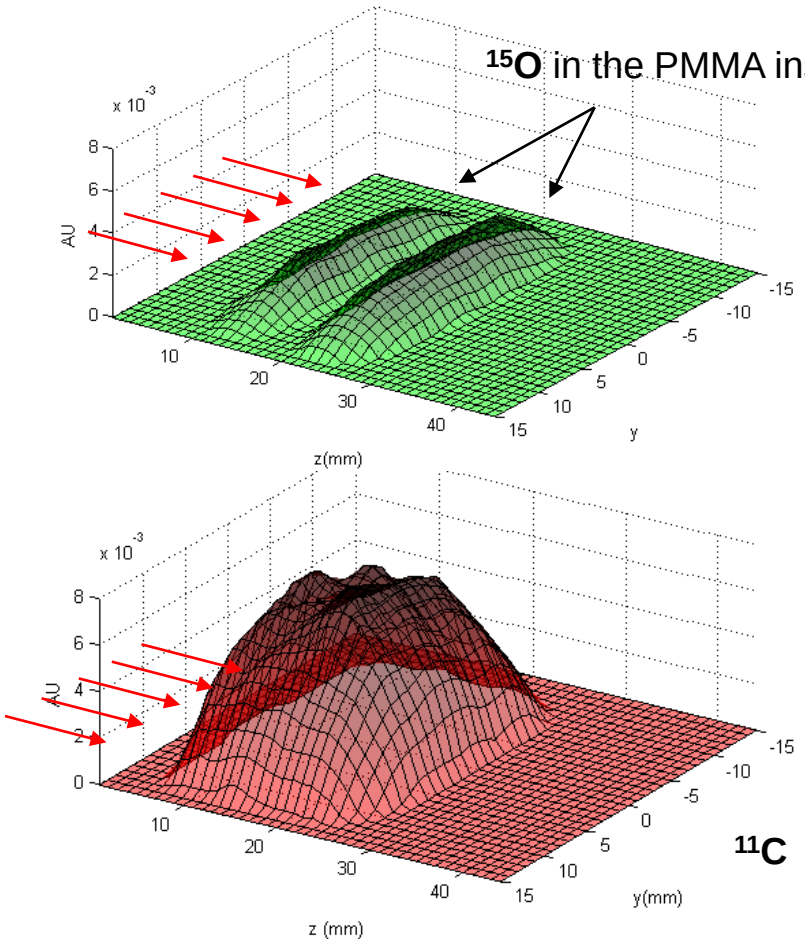

PE $^{12}\mathrm{C}\,(\mathrm{p},\mathrm{pn})^{11}\mathrm{C}$

PMMA $^{12}\mathrm{C}\,(\mathrm{p},\mathrm{pn})^{11}\mathrm{C}$, $^{16}\mathrm{O}\,(\mathrm{p},\mathrm{pn})^{15}\mathrm{O}$

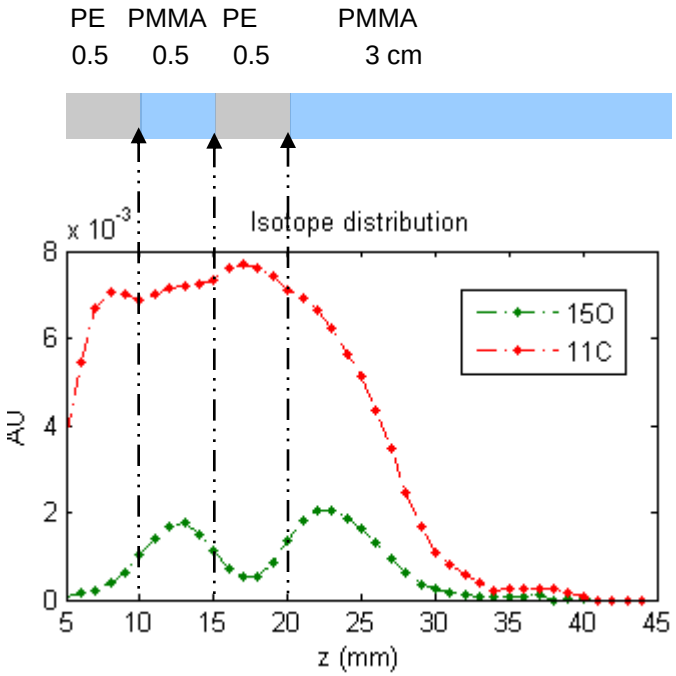

Exp#2: Validation of an analytical 1D filtering of the dose distribution for the calculation of the expected PET distribution in proton therapy (1)

The method (on patient 3D data)

- **Treatment Planning** on Patient ➔ Obtain planned Dose for each voxel with a CT number
- **Convert the patient** 3-D matrix **to PMMA** matrix (according to local electron density)
- **Apply the filters** (pre-obtained in PMMA) to the dose for each voxel to obtain activity
  - All the filters for production of the various radioisotopes are applied independently ➔ the activity due to each radioisotope is obtained
- **Convert the PMMA** 3-D Matrix **back to Patient** 3-D matrix
- **Compare the activities** as obtained from the **filter** with the activities as obtained by the **Monte Carlo**
- **[Compare the activities** as obtained from the **filter** with the activities as obtained **experimentally** – still to be done**]**

Validation of an analytical 1D filtering of the dose distribution for the calculation of the expected PET distribution in proton therapy (2)

The materials

Figure shows the MC depth-dose and positron emitter distributions used to calculate the reaction-dependent filter functions. All profiles were obtained integrating over the lateral field extension the distributions generated with the FLUKA code for $5x10^4$ protons stopped in a homogeneous target of polymethyl methacrylate (PMMA, $C_5H_8O_2$, ρ=1.18 g cm^{-3}) at the intermediate energy of 152.1 MeV (see left side).

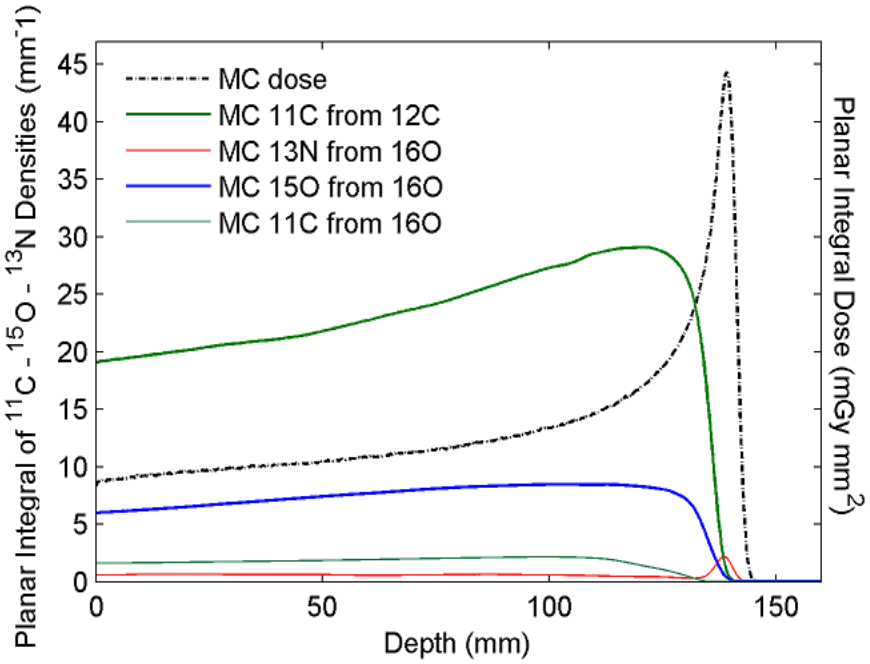

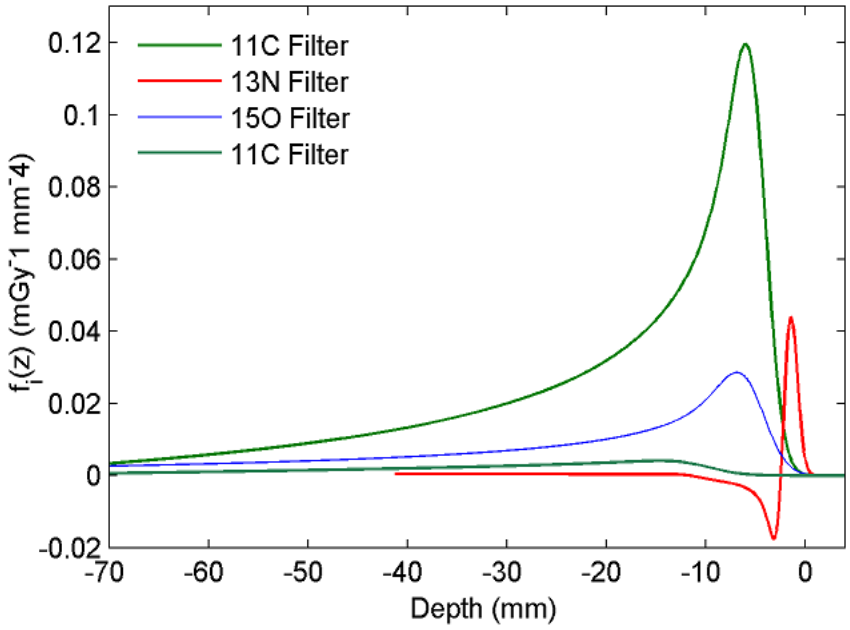

A Patient study: Filter predictions of β^+ - activity distribution vs CT-based Monte Carlo simulated patient data

Head and neck tumor sites
Case #1

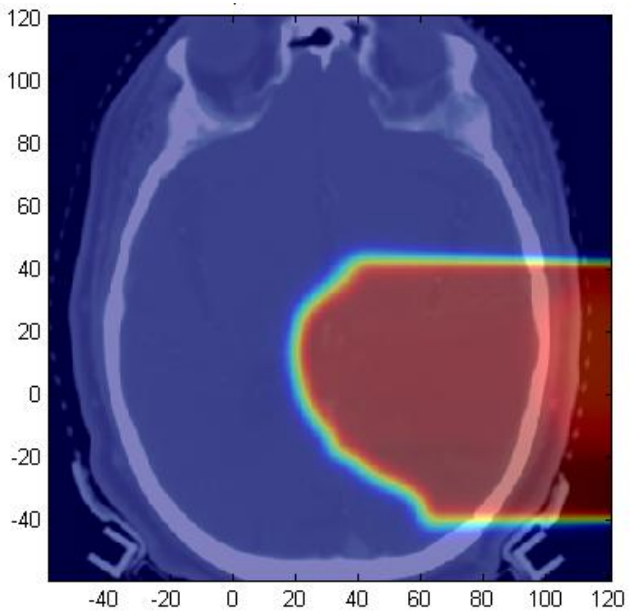

Input files :
The CT patient data and the prescribed dose distribution
Input parameters:
Voxel_ct dimensions in mm (x,y,z)
Voxel_plan_dose dimensions in mm (x,y,z)
Prescribed dose in mGy: 1 Gy
Duration of Irradiation: 75 s
Delay between irradiation and imaging: 10 s
Duration of imaging: 20 min

RESULTS : ^{11}C Filter prediction vs CT-based Monte Carlo simulated patient data

Head and neck tumor sites

At positions where the beam stopped in soft tissue

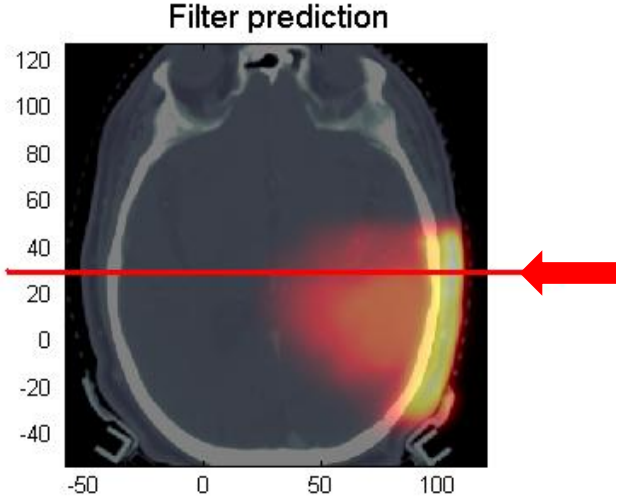

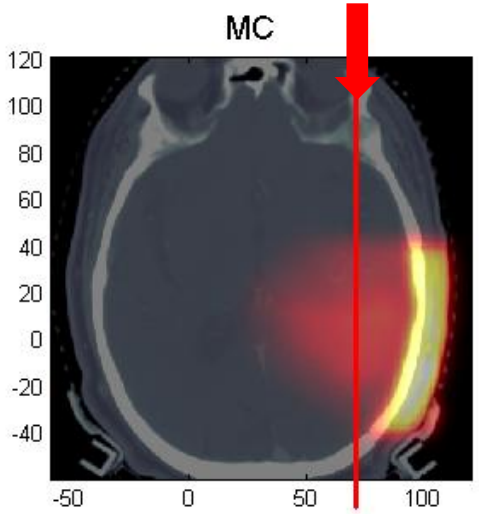

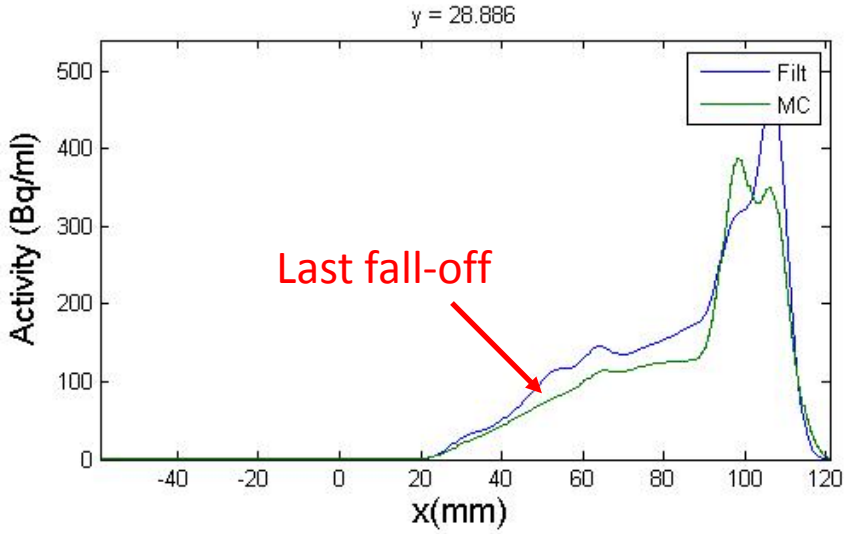

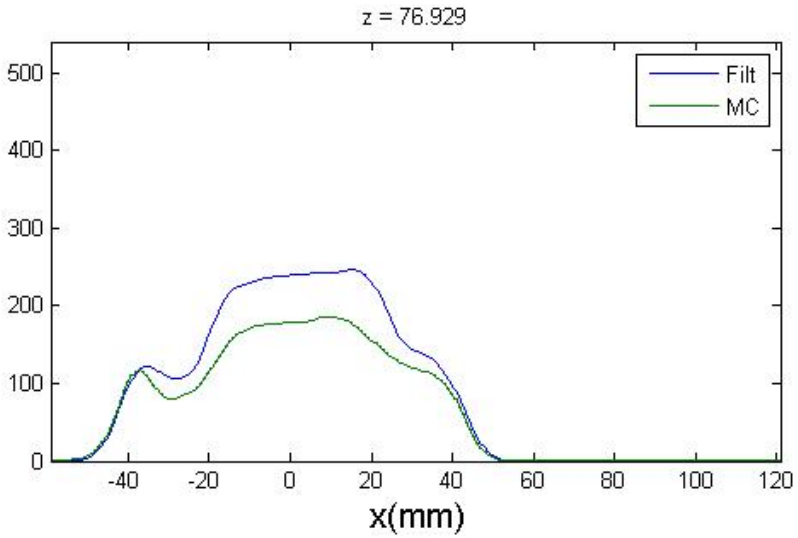

RESULTS : ^{15}O Filter prediction vs CT-based Monte Carlo simulated patient data

Head and neck tumor sites

At positions where the beam stopped in soft tissue

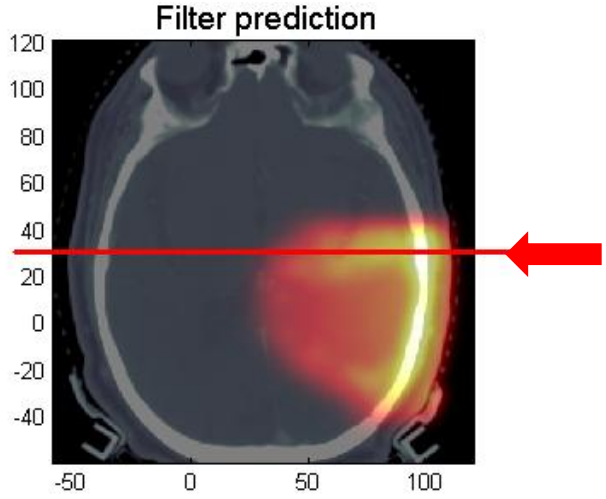

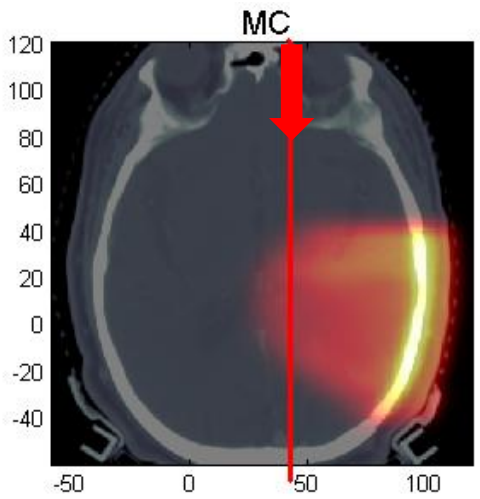

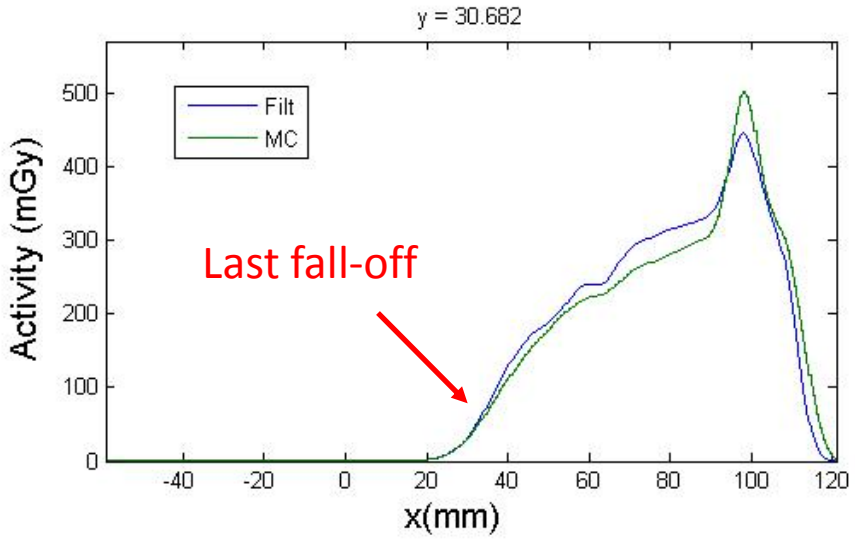

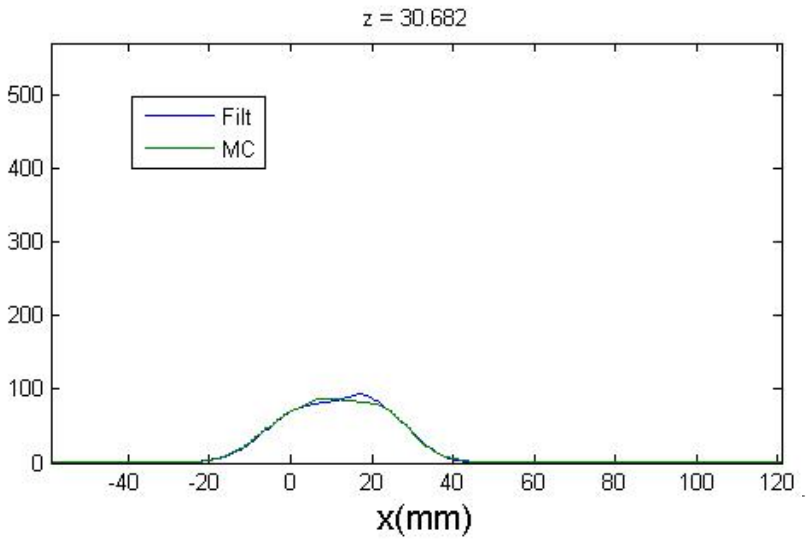

CONCLUSIONS

Five Technologies Set to Change the Decade* *(2009 - 2019)*

- **Building-Integrated Photovoltaics (BIPV)**
  - ***(solar technology projected to generate 50% of the electrical needs of the developing countries)***
- **Personal Genome Sequencing**
- **Molecular Imaging**
- **Graphene Transistors**
  - ***(nanomaterial graphene to replace silicon flash memory chips)***
- **Multi-touch Displays**

Wolf, J. Five Technologies Set to Change the Decade.* ***Forbes.com. Jan. 1, 2009*

[Courtesy of Hedvig Hricak, Memorial Sloan-Kettering Cancer Center, ECR-2009]

From WIKIPEDIA ➔Tomography

Atom probe tomography (APT)
- **Computed tomography (CT)**

Confocal laser scanning microscopy (LSCM)
Cryo-electron tomography (Cryo-ET)
Electrical capacitance tomography (ECT)
Electrical resistivity tomography (ERT)
Electrical impedance tomography (EIT)
Functional magnetic resonance imaging (fMRI)
Magnetic induction tomography (MIT)
- **Magnetic resonance imaging (MRI)**

Neutron tomography
Optical coherence tomography (OCT)
Optical projection tomography (OPT)
Process tomography (PT)
- **Positron emission tomography (PET)**
- **Positron emission tomography - computed tomography (PET-CT)**

Quantum tomography
- **Single photon emission computed tomography (SPECT)**

Seismic tomography
Ultrasound assisted optical tomography (UAOT)
Ultrasound transmission tomography
Photoacoustic tomography (PAT), also known as Optoacoustic Tomography (OAT)
Zeeman-Doppler imaging, used to reconstruct the magnetic geometry of rotating stars.

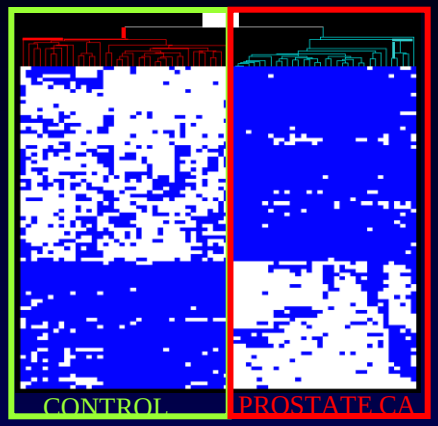

Proteomics

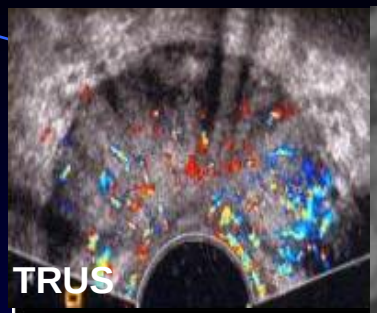

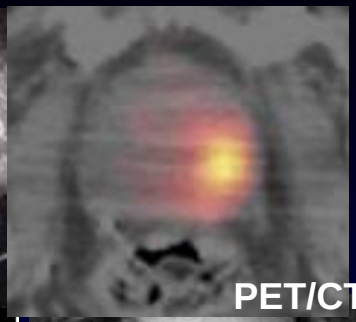

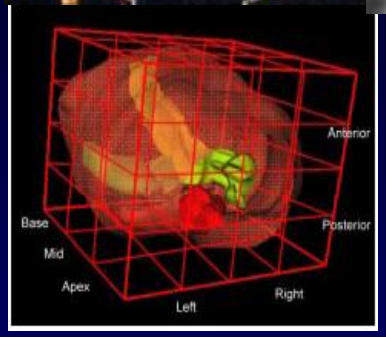

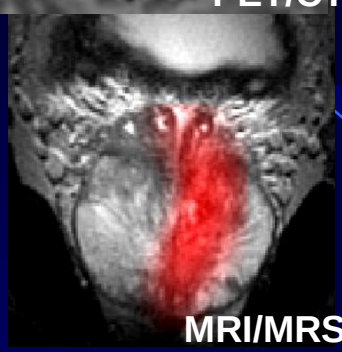

Imaging Prostate Cancer

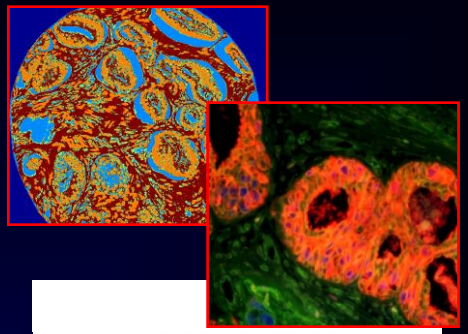

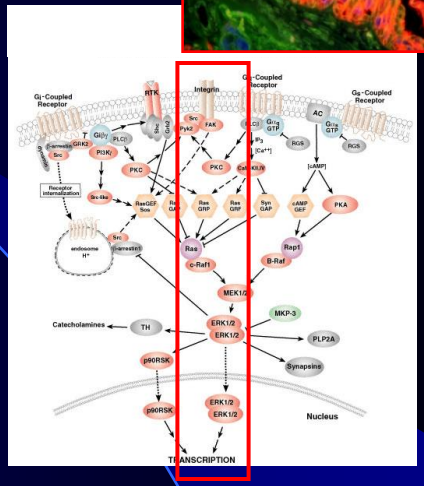

Molecular Pathway Identified & Targeted

Serum Screening

INTEGRATED DIAGNOSTICS APPROACH TO MANAGEMENT OF CANCER

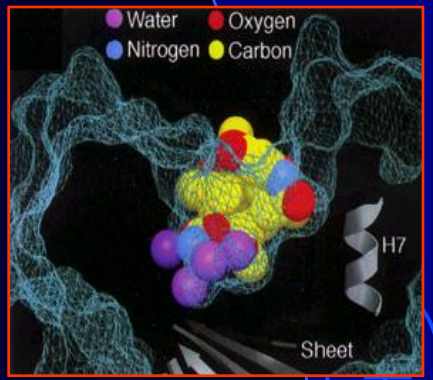

[Courtesy of Hedvig Hricak, Memorial Sloan-Kettering Cancer Center, ECR - 2009]

Prostate Cancer: Imaging Tumor Biology

Detection of metastasis: Targeted Imaging

^{99}Tc – Bone Scan

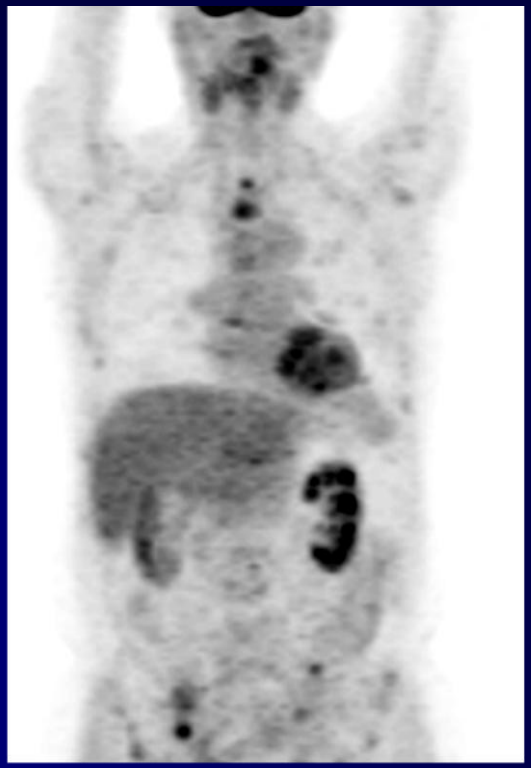

^{18}FDG PET

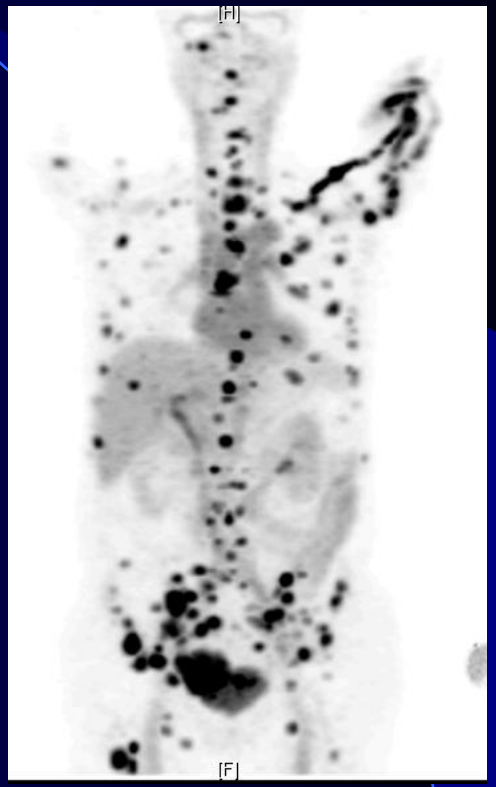

^{18}FDHT PET

Heiko Schoder: MSKCC

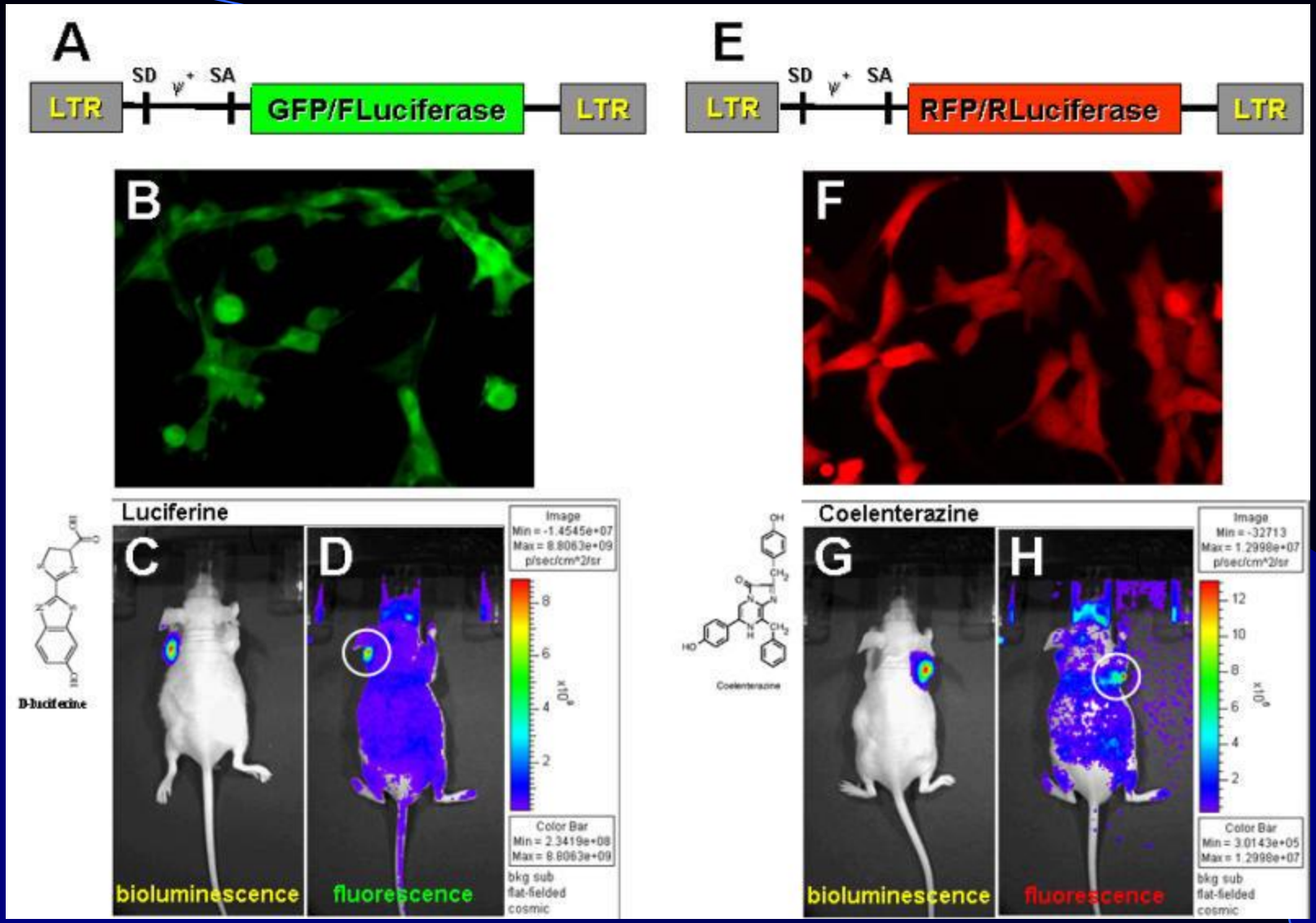

Multi-modality imaging of GFP/Firefly Luciferase and RFP/Renilla Luciferase Reporter Genes expression performed sequentially in the same living mouse in vivo

Hedvig Hricak, MSKCC

Acknowledgements #1

Many of the slides have been kindly provided by:

Thomas Beyer, CMI-experts, Zurich, Switzerland

Adrian Carpenter, WBIC, Univ Cambridge, UK

Simon Cherry, UC Davis, USA

Federica Fioroni, Reggio Emilia, Italy

Hedvig Hricak, MSKCC, New York, USA

Willi Kalender, Erlangen, Germany

Mike Phelps, UCLA, USA

Berndt Pichler, Tubingen, Germany

Group Collaborations:

INFN-DASIPM2, PRIN 2007 SipmPET

Collaboration with Institutions:

ISE srl (Pisa),FBK-isrt (Trento), LAL (Orsay), Univ Cambridge,

Pol Madrid, Univ Valencia, ...

Functional Imaging and Instrumentation Group
Department of Physics"E.Fermi"
University of Pisa and INFN, Pisa, Italy

Francesca Attanasi (PhD student)
Antonietta Bartoli (Post-doc)
Nicola Belcari (Researcher)
Valter Bencivelli (Associate Professor)
Laura Biagi (Post-doc)
Maria G. Bisogni (Assistant Professor)
Daniel Bonifacio (PhD Student)
Alberto Del Guerra (Full Professor)
Sebnem Erturk (PhD Student)

Abolfazl Arabpour-Feribors (PhD Student)
Serena Fabbri (PhD Student)
Gabriela Llosá (Marie Curie Fellow)
Sara Marcatili (PhD Student)
Sascha Moehrs (Post-doc)
Daniele Panetta (PhD Student)
Michela Tosetti (Researcher)
Valeria Rosso (Associate Professor)
Sara Vecchio (Post-doc)

Further reading

- **A.Del Guerra ,"IONIZING RADIATION DETECTORS FOR MEDICAL IMAGING" World Scientific, Singapore, ISBN 981-238-674-2, 2004, pp.1-507.**

- **W.A.Kalender, "COMPUTED TOMOGRAPHY", 2nd revised edition Publicis, Erlangen, Germany, ISBN 3-89578-216-5,2005,pp.1-304.**

- **J.L.Humm, A.Roszenfeld, A.Del Guerra,"From PET Detectors to PET Scanners. A Review", European Journal of Nuclear Medicine 30 (2003) 1574-1597.**

- **Tom K Lewellen, "Recent developments in PET detector technology", *Physics in Medicine and Biology* 53 (2008) R287-R317**

- **D.W.Townsend,"Multimodality imaging of structure and function", Physics in Medicine and Biology 53 (2008) R1- R39**

- **Berndt Pichler and Thomas Beyer (Guest Editors), "Multi-modality imaging: PET/MR", European Journal of Nuclear Medicine and Molecular Imaging, Vol 36 (Suppl 1) March 2009**

ANATOMY LECTURE ~ 2009 – MOLECULAR

[Courtesy of Hedvig Hricak, Memorial Sloan-Kettering Cancer Center, ECR-2009]

THE END